Redox Biology 34 (2020) 101547

Contents lists available at ScienceDirect

Redox Biology

journal homepage: www.elsevier.com/locate/redox

Research Paper

The mitochondrial peroxiredoxin displays distinct roles in different developmental stages of African trypanosomes

Marta Bogacz, Natalie Dirdjaja, Benedikt Wimmer, Carina Habich, R. Luise Krauth-Siegel*

Biochemie-Zentrum der Universität Heidelberg, Im Neuenheimer Feld 328, 69120, Heidelberg, Germany

ARTICLE INFO

Keywords:
Peroxiredoxin
Tryparedoxin
Trypanothione
Trypanosoma brucei
Mitochondrion
roGFP2

ABSTRACT

Hydroperoxide reduction in African trypanosomes relies on 2-Cys-peroxiredoxins (Prxs) and glutathione peroxidase-type enzymes (Pxs) which both obtain their reducing equivalents from the trypanothione/tryparedoxin couple and thus act as tryparedoxin peroxidases. While the cytosolic forms of the peroxidases are essential, the mitochondrial mPrx and Px III appear dispensable in bloodstream *Trypanosoma brucei*. This led to the suggestion that in this developmental stage which is characterized by a mitochondrion that lacks an active respiratory chain, only one of the two peroxidases might be required. Here we show that bloodstream cells in which the Px III gene is deleted and mPrx is down-regulated by RNA interference, proliferate as the parental cells indicating that both mitochondrial peroxidases are dispensable. However, when we raised the culture temperature to 39 °C, mPrx-depleted cells died indicating that under conditions mimicking a fever situation in the mammalian host, the protein becomes essential. In contrast, depletion of mPrx in insect stage procyclic *T. brucei* causes a proliferation defect under standard conditions at 27 °C, in the absence of any stress. In the absence of mPrx, a tryparedoxin-coupled roGFP2 biosensor expressed in the mitochondrial matrix is unable to respond to antimycin A treatment. Thus mPrx reduces mitochondrial H_2O_2 with the generation of trypanothione disulfide and acts as peroxidase. However, mPrx-depleted procyclic cells neither display any alteration in the cytosolic or mitochondrial trypanothione redox state nor increased sensitivity towards exogenous oxidative stressors suggesting that the peroxidase activity is not the crucial physiological function. After prolonged mPrx-depletion, the cells almost stop proliferation and display a highly elongated shape and diminished MitoTracker Red staining. In contrast to the situation in the mammalian bloodstream *T. brucei* and *Leishmania*, mPrx appears to play a constitutive role for the morphology, mitochondrial function and proliferation of the insect stage of African trypanosomes.

1. Introduction

Peroxiredoxins (Prxs) are ubiquitous and abundant proteins. Originally discovered as highly efficient reductases of H_2O_2, peroxynitrite and a wide range of organic hydroperoxides, Prxs are now known to play important roles in cellular redox signaling relays and also as chaperones (for recent reviews see Ref. [1–3]. As demonstrated for the cytosolic Prx1 and Prx2 in yeast, the proteins act as both peroxidases and thiol-independent molecular chaperones. Under oxidative stress or heat shock conditions, Prx1 is hyper-oxidized and forms high molecular weight complexes which lack peroxidase activity but act as super-chaperone [4].

Trypanosomatids are the causative agents of African sleeping sickness and Nagana cattle disease (*Trypanosoma brucei* species), Chagas' disease (*T. cruzi*) and the various forms of leishmaniasis (*Leishmania* species). African trypanosomes are obligate extracellular parasitic protozoa that multiply as bloodstream (BS) form in the mammalian host and as procyclic (PC) form in the tsetse fly vector. BS *T. brucei* rely on glycolysis for energy supply whereas the PC stage has a fully elaborated mitochondrion and gains ATP via oxidative phosphorylation. All trypanosomatids lack glutathione reductases and thioredoxin reductases but have a thiol redox metabolism that is based on trypanothione [N^1, N^8-bis(glutathionyl)spermidine, $T(SH)_2$)] and the flavoenzyme trypanothione reductase (TR) [5–8]. The trypanothione system delivers the reducing equivalents for a wide variety of essential pathways. In most of the reactions, tryparedoxin (Tpx), a thioredoxin-like oxidoreductase, catalyzes the electron transfer from $T(SH)_2$ onto the respective target protein [6–8].

Trypanosomes lack catalase. Hydroperoxides are detoxified by Prxs [9,10] and non-selenium glutathione peroxidase-type (Px) enzymes

* Corresponding author. Biochemie-Zentrum der Universität Heidelberg, Im Neuenheimer Feld 328, D-69120, Heidelberg, Germany.
E-mail address: luise.krauth-siegel@bzh.uni-heidelberg.de (R.L. Krauth-Siegel).

https://doi.org/10.1016/j.redox.2020.101547
Received 11 March 2020; Received in revised form 11 April 2020; Accepted 20 April 2020
Available online 29 April 2020

Abbreviations:

BS	bloodstream
cPrx	cytosolic 2-Cys-peroxiredoxin
KO	knockout
LipDH	lipoamide dehydrogenase
mPrx	mitochondrial 2-Cys-peroxiredoxin
PC	procyclic
Px	glutathione peroxidase-type tryparedoxin peroxidase
RNAi	RNA interference
SKO	single knockout
T. brucei	Trypanosoma brucei
T. cruzi	Trypanosoma cruzi
Tpx	tryparedoxin
Tpx-roGFP2	tryparedoxin-coupled redox sensitive green fluorescent protein 2
mito-roGFP2-Tpx	roGFP2-Tpx sensor with mitochondrial targeting sequence
Tet	tetracycline
TR	trypanothione reductase
Trx	thioredoxin
$T(SH)_2$	trypanothione
TS_2	trypanothione disulfide
WT	wildtype

[10–12]. Whereas the latter enzymes preferably detoxify lipid-derived hydroperoxides [13–15], the Prxs use hydrogen peroxide and peroxynitrite as main substrates [16,17]. Both types of peroxidases obtain their reducing equivalents from the $T(SH)_2$/Tpx couple and thus act as tryparedoxin peroxidases [6,8,11,18,19].

In *T. brucei*, three virtually identical Px-type enzymes are localized in the cytosol (Px I and II) and mitochondrion (Px III). RNA-interference against the peroxidases, which depletes all three proteins simultaneously, results in a severe growth defect in both BS and PC *T. brucei* [10,12]. Proliferation can, however, be fully restored by the presence of the vitamin E-analog Trolox [13–15,20]. Specific replacement of the genes encoding either the cytosolic or the mitochondrial forms, revealed that the cytosolic enzymes protect the cells from a lethal iron-mediated lysosomal damage [15], whereas the mitochondrial Px III is dispensible in BS *T. brucei* [14]. PC *T. brucei* lacking the Px-type enzymes undergo a ferroptosis-like cell death that probably originates at the mitochondrion [13,20].

All trypanosomatid Prxs characterized to date are typical 2-Cys-Prxs. Two different enzymes occur in the cytosol (cPrx) and mitochondrion (mPrx) [9,10,21,22]. Overexpression of cPrx or mPrx in epimastigote *T. cruzi* confers resistance against H_2O_2 and peroxynitrite [23]. *L. infantum* overexpressing cPrx present increased resistance to H_2O_2 whereas mPrx-overexpressing cells show significant resistance to *tert*-butyl hydroperoxide, but not H_2O_2 [16]. Overexpression of cPrx in *L. donovani* improves the capability of the parasites to cope with a combination of H_2O_2 and nitric oxide and results in increased virulence [24]. *L. donovani* overexpressing mPrx are protected against H_2O_2-induced programmed cell death, but have WT sensitivity towards exogenous oxidative stressors. The physiological role of mPrx has been proposed to be stabilization of the mitochondrial membrane potential and, as a consequence, inhibition of programmed cell death [25]. Promastigote *L. infantum* that lack mPrx are indistinguishable from WT cells under standard culture conditions but are unable to thrive in a murine model of infectivity [26]. The impaired virulence is not due to the lack of peroxidase activity but rather to the absence of a critical role played by mPrx as a molecular chaperone [26–28]. A thiol-independent chaperone activity has been reported also for *T. cruzi* cPrx [29].

RNAi against cPrx results in the lysis of BS *T. brucei* [10]. As shown recently, BS *T. brucei* deficient in DNA-repair highly express cPrx when exposed to NO. The authors suggest that the early immune response of the host enhances the activation of genes required to counteract oxidative stress and especially oxidative DNA damage [30]. In contrast, mPrx does not seem to play an essential role in the mammalian stage [10], and its function in the insect stage has not yet been investigated.

Here we report on the role of mPrx in the mammalian BS and insect PC stages of *T. brucei*. We show that under standard culture conditions, both mitochondrial tryparedoxin peroxidases are dispensable in BS cells, but under heat stress, mPrx is required for cell viability. In contrast, mPrx plays a role for the proliferation, cell morphology and maintainance of the mitochondrial membrane potential in the insect stage parasites.

2. Material and methods

2.1. Material

Tetracycline (Tet), 4′,6-diamino-2-phenylindole (DAPI), diamide, N-ethylmaleimide (NEM), 2′,7′-dichlorofluoresceine diacetate (DCFH-DA), dimethyl pimelimidate (DMP), carbonyl cyanide 4-(trifluoromethoxy)phenylhydrazone (FCCP), ethanolamine and lipoamide were purchased from Sigma-Aldrich. MitoTracker Red CMXRos and MitoTracker Green were from Life Technologies. Hydrogen peroxide (30%) was from Merck. Hygromycin B and geneticin disulfate (G418) were purchased from Roth. Protein A-agarose (#20333) was from Pierce Biotechnology. MitoParaquat (ab146819) and rabbit anti-peroxiredoxin-SO_3 antibodies (ab16830) were from Abcam. Recombinant *T. brucei* trypanothione reductase (TR), tryparedoxin (Tpx), glutathione peroxidase-type tryparedoxin peroxidase (Px) [13], thioredoxin (Trx) [31], lipoamide dehydrogenase (LipDH) [32] and human glutathione reductase (hGR) [33] were prepared as described. Trypanothione ($T(SH)_2$) and trypanothione disulfide (TS_2) were generated enzymatically [13]. Polyclonal rabbit antibodies against *T. brucei* cPrx [34], Tpx [12] and LipDH [32] and guinea pig antibodies against mPrx [35] were obtained previously. Polyclonal rabbit antibodies against *T. cruzi* TR were generated by Eurogentec. HRP-conjugated goat anti-rabbit IgGs were ordered from Santa Cruz Biotechnology and HRP-conjugated donkey anti-guinea pig IgGs from Thermo Scientific. Alexa Fluor 488-conjugated goat anti-guinea pig IgGs were from Life Technologies. The pHD678 plasmid was a kind gift from Dr. Christine Clayton, Heidelberg, Germany. The pETtrx1b plasmid, encoding an N-terminal TEV-protease cleavable thioredoxin-His_6 tag, was provided by Gunther Stier, Heidelberg.

2.2. Cloning, expression and purification of recombinant T. brucei mPrx

The full-length *mprx* coding region (Tb427.08.1990) was amplified from genomic DNA isolated from PC *T. brucei* by PCR using mprx_fw (5′-CATTCCATGGGACTTCGCCGTTTCTC-3′) and mprx_rev (5′-CTGGGTACCCTATAGATTCTTCTC-3′) as primers and Taq polymerase. The amplicon was cloned into the pGEM®-T vector (Promega) following the manufacturer's instructions and transformed into Nova blue singles™ competent cells (Novagen). The plasmid was sequenced (GATC-Eurofins Genomics) and used as template to amplify *T. brucei mprx* without mitochondrial targeting sequence (mts) with mprx-mts_fw (5′-CAGCCATGGGAAACCTCGACTATC-3′) and mprx_rev as primers. The PCR product was treated with DpnI for 90 min at 37 °C, digested with NcoI and Acc65I (ThermoScientific), gel purified and cloned into pETtrx1b. The plasmid was amplified in Nova blue singles™ cells and sequenced.

E. coli BL21 (DE3) competent cells (Novagen) were transformed with the purified pETtrx1b*mprx-mts* plasmid. Cells from a 3 l recombinant bacterial culture were induced with 0.2 mM IPTG (Peqlab) at an OD_{600nm} of about 0.6, overnight cultured at 18 °C and 180 rpm

and harvested. The pellet was resuspended in 50 ml 50 mM NaH_2PO_4, 300 mM NaCl, pH 7.5 (buffer A) containing 50 μM PMSF, 150 nM pepstatin, 4 nM cystatin, 5 mg lysozyme (Calbiochem) and 0.5 mg of DNase A (Calbiochem) and the cells were disintegrated by sonification. After centrifugation, the supernatant was loaded on a 5 ml Ni-NTA Superflow column (Qiagen). The column was washed with 10 vol of buffer A containing 10 mM imidazole and the fusion protein eluted by a gradient from 10 mM to 250 mM imidazole in 120 min at a velocity of 1 ml/min. Peak fractions were pooled, and the buffer was exchanged to buffer A in an Amicon® Ultra-15 concentrator with a cut-off of 10 kDa (Sigma-Aldrich Merck-Millipore). After overnight incubation at 4 °C with His-tagged TEV protease, the digest was applied onto a second Ni-NTA column. Peak fractions were treated as described above and stored at 4 °C with addition of 0.02% sodium azide. Purity of the recombinant tag-free *T. brucei* mPrx was verified by SDS-PAGE.

2.3. In vitro peroxidase assays

The assays were performed in a total volume of 200 μl of 100 mM Tris, 5 mM EDTA, pH 7.6 (Px-buffer), unless stated otherwise. The reactions were started by adding 50 μM H_2O_2 and NADPH or NADH consumption was followed at 340 nm and 25 °C. The trypanothione/Tpx-dependent peroxidase activity was measured in the presence of 240 μM NADPH, 90 μM TS_2, 200 mU TR, 0 or 10 μM Tpx and 0.3–2 μM mPrx. To follow a putative glutathione peroxidase activity, the assays were conducted in 100 mM Tris/HCl, 5 mM EDTA, pH 8.0 [36] containing 200 μM NADPH, 0.5–2.8 U hGR, 3 mM GSH, and 10.8 μM mPrx. Reliability of the assay was confirmed by adding bovine erythrocyte glutathione peroxidase (Sigma) which yielded activities of > 4000 U/mg. The ability of lipoamide to act as reducing substrate of Tpx or mPrx was measured in assays with 200 μM NADH, 300 μM pre-reduced lipoamide [37], 200 mU LipDH, 0 or 10 μM Tpx and 0.15–0.3 μM mPrx. To evaluate the ability of Trx to replace Tpx, the trypanothione/Tpx assays were conducted in the presence of 150 μM NADPH, 300 μM $T(SH)_2$, 200 mU TR with either 11 μM Trx alone or with both, 11 μM Trx and 10 μM Tpx, and 0.11–0.32 μM mPrx.

2.4. Cultivation of T. brucei

All cells used in this work were culture-adapted *Trypanosoma brucei brucei* 449 (Lister strain 427) that stably express the tetracycline repressor [38]. BS and PC cells were cultivated in HMI-9 medium at 37 °C and MEM-Pros medium at 27 °C, respectively, as described before [12,13]. BS Px III KO cells were generated previously [14]. PC *T. brucei* constitutively expressing Tpx-roGFP2 or mito-roGFP2-Tpx were generated recently and kept in presence of 30 μg/ml G418 [33]. BS and PC mPrx RNAi cells were constantly cultured in the presence of hygromycin (10 and 50 μg/ml, respectively) to ensure maintenance of the integrated pHD678_*mprx* construct (see sections 2.5. and 2.6.). Notably, under standard culture conditions, the parasites showed virtually the same proliferation as the respective WT parasites grown without hygromycin.

2.5. Cloning of a hairpin construct for inducible RNAi against mPrx in T. brucei

The pHD678 plasmid contains a hygromycin resistance gene and allows for Tet-inducible RNAi against a target mRNA. Two fragments of the *mprx* coding sequence were amplified from *T. brucei* genomic DNA, a 301 bp fragment using primers 5′-GCGAAGCTTGGACGGAAAGATCAAGG-3′ and 5′-CACAGTACGCGTTCTTCGACCAACACC-3′, and a 366 bp fragment covering the sequence of the short fragment plus additional 65 bp, using primers 5′-GCAGGGATCCGGACGGAAAGATCAAGG-3′ and 5′-GCAAATACGCGTTGGTCACATGGCGAAG-3’ (restriction sites underlined). The short amplicon, long amplicon and pHD678_*px3* [39] were digested with *Hind*III/*Mlu*I, *BamH*I/*Mlu*I and *Hind*III/*BamH*I, respectively, purified and ligated yielding pHD678_*mprx*.

2.6. Generation and phenotypical analysis of mPrx RNAi cells

BS WT and Px III KO, as well as PC WT cells were transfected with the *Not*I-linearized plasmid pHD678_*mprx*. After 24 h cultivation, hygromycin was added, and resistant clones were selected by serial dilutions essentially as described before [35]. To induce RNAi, logarithmically growing cells were transferred into medium containing 1 μg/ml Tet. If not stated otherwise, for phenotypical analyses, the density was adjusted to 1.5–2 (BS) or 5 (PC) x 10^5 cells/ml. Every 24 h, living parasites were counted in a Neubauer chamber and the cultures diluted back to the starting density. All phenotypic analyses of the mPrx RNAi cells were conducted in the presence of hygromycin (section 2.4.).

To follow the heat sensitivity of BS cells, mPrx RNAi cells were cultured ± Tet for 48 h under standard conditions at 37 °C. Subsequently, the cells were either kept at 37 °C or transferred to 39 °C and proliferation was followed for another three days. WT cells + Tet were treated accordingly. For the phenotypical analyses of PC cells, the mPrx RNAi cells were grown for various days ± Tet. Mito-paraquat (10 mM in DMSO), H_2O_2 (9.8 M) or antimycin A (10 mM in DMSO) was added to the cultures at varying concentrations. For heat stress experiments, the PC parasites were grown in parallel at 27 °C and 37 °C. To study the effect of high glucose on the proliferation of mPrx-depleted PC cells, the cells were pre-cultured ± 10 mM glucose without Tet for seven days. Subsequently, the cells were split into medium ± 10 mM glucose ± Tet at a density of 5 × 10^5 cells/ml, and cell growth was followed for 10 days. Every 24 h, living cells were counted and the culture was diluted back to the starting density with fresh medium ± glucose ± Tet. PC WT parasites cultured ± 10 mM glucose served as control.

2.7. Immunofluorescence microscopy

About 1.2 × 10^6 cells were used per condition. PC mPrx RNAi cells were cultured with Tet for three and seven days. Non-induced parasites served as controls. Staining with MitoTracker Red, as well as cell fixation, permeabilization and incubation with antibodies were performed as described [15,20]. The anti-mPrx, anti-LipDH, Alexa Fluor 488 goat anti-guinea pig IgGs and anti-rabbit IgGs antibodies were diluted 1:1000. DAPI (50 μg/ml) was used for visualization of the nuclear and kinetoplast DNA. Samples were imaged using a Carl Zeiss Axiovert 200 M widefield microscope equipped with an AxioCam MRm digital camera and the AxioVision software (Zeiss, Jena, Germany).

2.8. Flow cytometry

All treatments were performed at 27 °C in the dark. PC mPrx RNAi cells were cultured ± Tet for three or seven days. About 1.1 × 10^6 cells were centrifuged, washed with 1 ml ice-cold PBS, re-suspended in 1 ml medium ± MitoTracker Red or Green (0.12 μM) and incubated for 15 min. Next, the cells were washed with 1 ml ice-cold PBS, re-suspended in 1 ml medium and incubated for 30 min. For control, staining and post-staining incubations were performed in medium supplemented with 20 μM FCCP. To measure cellular oxidative stress, PC WT cells and mPrx RNAi cells cultured ± Tet for three or seven days were washed with 1 ml ice-cold PBS, re-suspended in 1 ml medium containing 500 μM H_2O_2 and incubated for 30 min. Subsequently, the cells were washed with 1 ml ice-cold PBS, re-suspended in 1 ml medium ± 10 μM DCFH-DA and incubated for 30 min. Afterwards, the cells were washed with 1 ml ice-cold PBS, re-suspended in 1 ml ice-cold PBS, transferred into FACS tubes (Sarsted) and immediately analyzed on the FACS Canto flow cytometer at the Flow Cytometry and FACS Core Facility (FFCF) of the Center of Molecular Biology (ZMBH) of Heidelberg University. Data were collected using the 561:586/15 nm (ex:em) laser (MitoTracker Red) and the 488:530/

30 nm laser in the case of MitoTracker Green and DCF. In each experiment, 10000 events were recorded. The data were analyzed using FlowJo software (FlowJo, LLC).

2.9. Western Blot analyses

Total lysates of the different BS and PC cell lines were subjected to SDS-PAGE using 12% gels, if not otherwise stated, and the proteins blotted onto PVDF membranes. The membranes were probed with antibodies against mPrx (1:3000), cPrx (1:3000), Tpx (1:2000), LipDH (1:1000) and TR (1:1000), followed by HRP-conjugated donkey anti-guinea pig IgGs (1:15000) or goat anti-rabbit IgGs (1:20000) antibodies. To follow hyper-oxidation of mPrx and cPrx, the membrane was probed with anti-Prx-SO_3 (1:1600)/anti-rabbit IgGs antibodies. For details, see the figure legends.

2.10. Plate-reader based fluorescence measurements of PC cells expressing roGFP2 biosensors

The measurements were performed using a PHERAstar FS plate reader (BMG Labtech) virtually as described [33]. Briefly, PC Tpx-roGFP2/mPrx RNAi and mito-roGFP2-Tpx/mPrx RNAi cells were cultured ± Tet for three or seven days. The mPrx RNAi cells kept without Tet served as fluorescence background control. The cells were harvested, washed and re-suspended in medium lacking hemin and phenol red. Aliquots of 200 µl were applied per well of a 96-well black/clear bottom imaging plate (BD Falcon), corresponding to 1×10^7 cells/well. For full sensor reduction and oxidation, 1 mM DTT and 3 mM diamide, respectively, was added. Antimycin A (10 mM in DMSO) was diluted to 200 µM with water. The cells were treated with 10 or 30 µM antimycin A or with 15 µl DMSO. The final DMSO content in each well was 0.3%. After excitation at 400 and 485 nm, emission at 520 nm was measured. The degree of sensor oxidation (OxD) was calculated following published procedures [40].

2.11. Immunoprecipitation of cPrx or mPrx from H_2O_2-stressed PC T. brucei

The IgGs from 2 ml of the cPrx and mPrx antisera were enriched by 33% ammonium sulfate precipitation over night at 4 °C and re-dissolved in PBS-T (PBS + 0.05% Tween). Two samples of 1 ml protein A-coated agarose slurry (approx. 500 µl beads) were washed twice with PBS and PBS-T by gentle rotation and centrifuged for 1 min at 2000 rpm at room temperature. The IgGs were added and the beads incubated for 1 h at 4 °C. After centrifugation, the beads were washed three times with PBS-T and once with 0.1 M sodium borate, pH 9.0. Next, the antibodies were cross-linked with protein A by 30 min incubation with 20 mM DMP (freshly prepared in 0.1 M sodium borate, pH 9.0) at room temperature. After centrifugation, the supernatant was removed and the cross-linking step repeated. To stop the reaction, the beads were incubated twice for 5 min with 0.1 M ethanolamine in PBS. After a wash with PBS, unbound antibodies were removed by two washes with cold 0.1 M glycine, pH 2.5. The beads were stored at 4 °C in PBS-T containing 0.02% sodium azide.

About 8×10^8 PC WT cells were treated for 5 min with 100 µM or 10 µM H_2O_2 at 23 °C, centrifuged, re-suspended in 20 mM NEM in PBS, lysed by freezing/thawing and centrifuged again. The supernatants were collected. An aliquot of 8×10^7 cells was boiled in SDS sample buffer with 2- mercaptoethanol. The remaining cell lysate was split into two parts (input), added to the anti-cPrx and anti-mPrx protein A-agarose beads and incubated for 4 h at 4 °C with gentle rotation. After centrifugation, the supernatants (flow through) were collected and the beads washed three times with 20 mM NEM in washing buffer (10 mM Tris, 1 mM EDTA, 150 mM NaCl, pH 7.4). Each time, the beads were centrifuged and the supernatants collected. Aliquots of each fraction (flow through, washes) and the beads were boiled for 10 min in SDS sample buffer with 2-mercaptoethanol. Extracts of 4×10^7 cells (10% of input), 10% of flow through, 5% of washes and the supernatant of the beads were loaded per lane and subjected to SDS-PAGE. After blotting, the PVDF membranes were probed with anti-Prx-SO_3/anti-rabbit IgGs antibodies. The membranes were stripped and probed with anti-cPrx/anti-rabbit IgGs antibodies in case of the immunoprecipitation of cPrx, or with anti-mPrx/anti-guinea pig IgGs antibodies in case of the mPrx immunoprecipitation. After re-activation in methanol, the membranes were reacted with antibodies against the respective other Prx as described above. As last step, both membranes were probed with anti-LipDH and anti-rabbit IgGs antibodies.

2.12. Analysis of protein aggregation

The formation of aggregated proteins was studied essentially following published procedures [27,41]. Briefly, about 5×10^7 cells were harvested and washed with 10 ml ice-cold lysis buffer (50 mM potassium phosphate, pH 7.0, 1 mM EDTA, 5% glycerol), centrifuged for 5 min at 2000 g and 4 °C, re-suspended in 200 µl lysis buffer and stored at −80 °C. The cells were thawn at 37 °C and disintegrated by five rounds of freezing/thawing, followed by 5 min sonication on ice. After 20 min centrifugation at 17,000 g and 4 °C, the supernatant was removed. The pellet was re-suspended in 400 µl lysis buffer containing 20% Nonidet-P-40, centrifuged again, and washed twice with 500 µl lysis buffer. Finally the pellet was dissolved in reducing sample buffer containing 4 M urea. The equivalent of 1×10^7 cells was loaded per lane of a 10% gel and subjected to SDS-PAGE.

3. Results

3.1. Recombinant T. brucei mPrx has tryparedoxin peroxidase activity

Recombinant *T. brucei* mPrx has been shown to reduce H_2O_2 in the TR/$T(SH)_2$/Tpx peroxidase assay, albeit with seven-fold lower activity than cPrx [9]. This led to the suggestion that another oxidoreductase may act as physiological partner of the mitochondrial peroxidase. Here we generated tag-free *T. brucei* mPrx without putative mitochondrial pre-sequence (Fig. S1A). Antibodies raised against the purified protein revealed a single strong band in lysates of both BS and PC *T. brucei* cells whose mass corresponded that of the recombinant mPrx and did not react with cPrx (Fig. S1B). The data showed that mPrx is an abundant protein in both developmental stages of the parasite, the mature authentic mPrx lacks approximately the first 26 residues, and the mPrx antiserum does not cross-react with cPrx.

Recombinant *T. brucei* mPrx was then subjected to peroxidase assays with H_2O_2 as substrate and various thiol systems as putative donors of reducing equivalents. The protein displayed an activity of 3.1 ± 0.3 U/mg in the TR/$T(SH)_2$/Tpx assay, but no activity in presence of GSH and human glutathione reductase (Table 1). $T(SH)_2$ can be replaced, albeit less efficiently, by lipoamide as electron donor for the mitochondrial *L. infantum* Tpx2 [42]. Indeed also *T. brucei* mPrx showed activity when the assay contained lipoamide and lipoamide dehydrogenase instead of the $T(SH)_2$/TR couple. However, in the absence of Tpx, no activity was observed indicating that lipoamide is unable to directly reduce mPrx. In addition, free lipoamide is unlikely to act as an efficient reducing agent due its low physiological abundance [42]. Thioredoxins (Trxs) are the most general electron donors for 2-Cys-Prxs [1]. *T. brucei* has a classical Trx which *in vitro* delivers electrons to the Px-type enzymes as well as *Crithidia fasciculata* Prx, but less efficiently when compared with Tpx [11,31]. The protein does not have an obvious mitochondrial pre-sequence and seems to be dispensable for *T. brucei* [43]. Nevertheless, a genome-wide localization study revealed N-terminally mNeonGreen-tagged Trx in the mitochondrion of PC *T. brucei* [44]. Therefore, we studied if the protein could act as oxidoreductase and transfer electrons from $T(SH)_2$ onto mPrx. When the reaction mixture contained Trx, but no Tpx, we did not detect any

Table 1
Peroxidase activity of *T. brucei* mPrx towards H_2O_2 in presence of various reducing systems.

Reducing system	Tpx [μM]	mPrx activity [U/mg]
$T(SH)_2$/TR	0	0
	10	3.1 ± 0.3
GSH/hGR	0	0
Lipoamide/LipDH	0	0
	10	1.2 ± 0.1
$T(SH)_2$/TR/Trx	0	0
	10	3.1 ± 0.2

The assays contained the respective reducing system ± 10 μM Tpx, as indicated. The reactions were started by adding H_2O_2. For details see section 2.3. The values represent the mean ± SD of at least three independent measurements. hGR, human glutathione reductase; LipDH, lipoamide dehydrogenase; Trx, thioredoxin.

peroxidase activity. In the presence of both oxidoreductases, the activity of mPrx corresponded to that of Tpx alone. The recently characterized mitochondrial Trx2 lacks any reductase activity [45]. None of the low molecular weight thiols studied directly reduced mPrx, and Trx was unable to replace Tpx. In the presence of Tpx, $T(SH)_2$ and also lipoamide are able to deliver electrons for the reduction of mPrx.

3.2. Both mitochondrial peroxidases are dispensable in BS T. brucei under standard culture conditions

Depletion of mPrx by RNAi does not cause a loss of fitness in BS trypanosomes [10]. Also the gene encoding Px III is dispensable [14]. To evaluate if one of the two mitochondrial peroxidases may be required, we transfected WT and Px III KO cells with a construct that allowed the Tet-inducible depletion of mPrx. WT parasites as well as Px III KO, mPrx RNAi and Px III/mPrx RNAi cell lines were then cultured in the presence and absence of Tet (Fig. 1A). Western blot analyses revealed the efficient down-regulation of mPrx already after one day of RNAi induction (Fig. 1B). All cell lines lacking Px III proliferated at a slightly reduced rate when compared to WT parasites, in accordance with previous data [14]. The simultaneous depletion of mPrx did not have any further effect on the proliferation (Fig. 1A). Under standard culture conditions, BS *T. brucei* do not appear to require any of the mitochondrial peroxidases.

3.3. Under heat stress, mPrx-depletion is lethal for BS T. brucei

In *L. infantum*, mPrx functions primarily as a heat-activated molecular chaperone [26–28]. To investigate if the protein might fulfill a similar role in BS stage *T. brucei*, the mPrx RNAi cells were pre-induced with Tet for 48 h and then cultured in parallel at 37 °C and 39 °C. Non-induced cells and WT parasites + Tet served as controls. The increased temperature severely affected the proliferation of all cells (Fig. 2A). However, in contrast to WT parasites and non-induced mPrx RNAi cells, which were still able to proliferate, the mPrx-depleted cells started to die after 48 h and were almost completely lysed after 72 h at 39 °C. Western blot analysis confirmed the efficient down-regulation of mPrx in the induced mPrx RNAi cell lines (Fig. 2B). It also revealed that the non-induced cells had a slightly lower level of the protein than WT parasites, presumably due to some leakiness of the RNAi construct. This, together with the fact that the experiments were conducted in presence of hygromycin, to retain the genomic integration of the RNAi construct, is likely the reason for the lower proliferation of the non-induced RNAi cell lines at 39 °C compared to WT parasites. The data indicate that BS parasites need mPrx for viability when they face a temperature that could occur during fever episodes of their mammalian host. One should, however, also consider that an adult cow has a body temperature of about 39 °C. The *T. brucei* Lister strain 427 used in this work was most probably isolated from an infected cattle (http://tryps.rockefeller.edu/DocumentsGlobal/lineage_Lister427.pdf), then propagated in mice with a body temperature of 37 °C and adapted to laboratory conditions. Thus, in their natural hosts, BS *T. brucei* may require mPrx even under physiological conditions.

3.4. PC T. brucei require mPrx for proliferation under standard culture conditions

Insect stage *T. brucei* possess a fully developed mitochondrion and generate ATP mainly by oxidative phosphorylation. As the role of mPrx in PC parasites has not been investigated so far, we generated cell lines that allowed Tet-inducible down-regulation of the protein. Cultivation of the mPrx RNAi cells in presence of Tet resulted in a significant proliferation defect, starting on day four (Fig. 3A). At day six, the cells duplicated only once per 24 h. This low growth rate persisted for another two to five days (depending on the clone). Afterwards, the proliferation gradually increased again and after ten (maximally 15) days

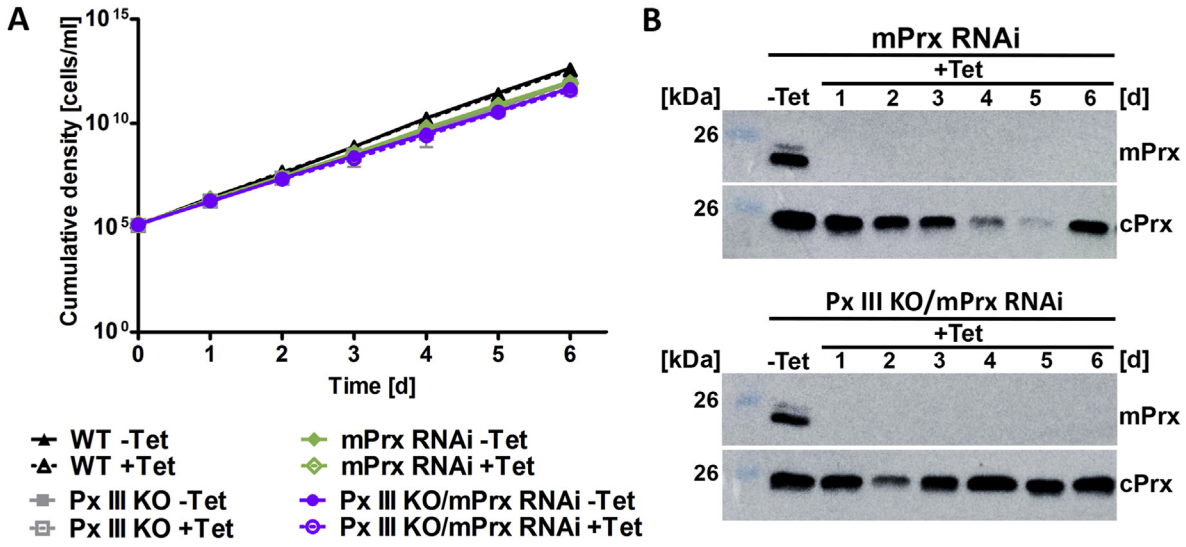

Fig. 1. BS trypanosomes lacking both mPrx and Px III proliferate almost as WT parasites. WT parasites as well as Px III KO, mPrx RNAi and Px III KO/mPrx RNAi cell lines were cultured ± Tet. (**A**) Cell proliferation was followed for six days. The data represent the mean ± SD from three independent experiments with one clone. Three other clones of both mPrx RNAi and Px III KO/mPrx RNAi cells were studied for three days and behaved identically. (**B**) Total lysates of 5×10^6 cells/lane were subjected to Western Blot analysis against mPrx and re-developed with antibodies against cPrx.

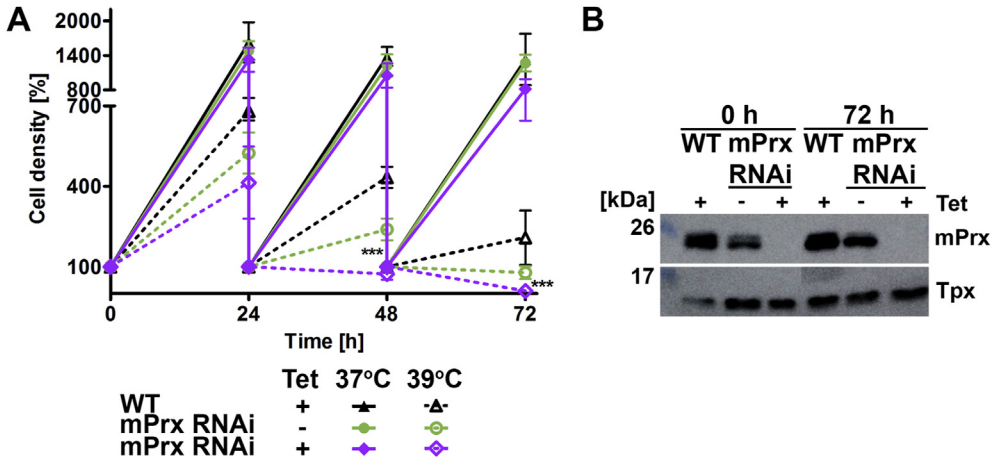

Fig. 2. BS *T. brucei* subjected to RNAi against mPrx do not survive prolonged exposure to 39 ˚C. BS mPrx RNAi cells were pre-cultured ± Tet for 48 h at 37 ˚C, transferred into two flasks with medium ± Tet and then cultured in parallel at 37 ˚C and 39 ˚C. WT parasites in medium + Tet were treated accordingly. (**A**) Every 24 h, viable cells were counted and the cultures diluted to the starting density of 2×10^5 cells/ml. The values are the mean ± SD from three independent experiments with two clones. The data for mPrx RNAi cells cultured at 39 ˚C in the absence (green dashed line) and presence (purple dashed line) of Tet were analyzed by a standard unpaired *t*-test (***, $p \leq 0.001$). (**B**) Cells cultured at 37 ˚C were collected at the start (0 h) and end (72 h) of the experiment. Total lysates of 2×10^6 cells/lane from one of the clones were subjected to Western Blot analysis with mPrx antibodies and re-developed with anti-Tpx antibodies. (For interpretation of the references to colour in this figure legend, the reader is referred to the Web version of this article.)

corresponded to that of non-induced cells. Western blot analyses revealed that mPrx was down-regulated 24 h after the onset of RNAi and virtually undetectable in cells induced for two to six days (Fig. 3B). Upon prolonged cultivation, the protein re-appeared despite the presence of Tet, in accordance with the observed restoration of normal growth (Fig. 3A). Such a loss of RNAi regulation is a phenomenon often observed for essential *T. brucei* proteins [35,45].

PC *T. brucei* reside in the midgut of the tsetse fly where they use proline as main substrate for energy production. However, in a glucose-rich environment, the parasites generate ATP primarily by glycolysis [46,47]. The medium we use to cultivate PC trypanosomes does not contain glucose except for the < 0.5 mM originating from the fetal calf serum [32]. To induce glycolysis, we cultured the mPrx RNAi cells in presence of 10 mM glucose for seven days and then transferred the cells into medium + glucose ± Tet (Fig. S2). The high glucose concentration had only a minor positive effect on the proliferation of the mPrx-depleted cells. A metabolic shift from oxidative phosphorylation to more glycolysis does not appear to effectively revert the proliferation defect of the mPrx-depleted PC parasites.

Remarkably, the growth arrest of the mPrx-depleted cells was accompanied by the appearance of thin and long cells (Fig. 3C). To get an insight if these morphological changes correlate with a specific cell cycle arrest, we inspected the cells for their kinetoplast (K) and nuclear (N) DNA content. Cells with non-dividing kinetoplast and a single nucleus (1K1N) are in the G1-phase. Trypanosomes with two kinetoplasts and one nucleus (2K1N) are in G2/M phase while parasites with 2K2N

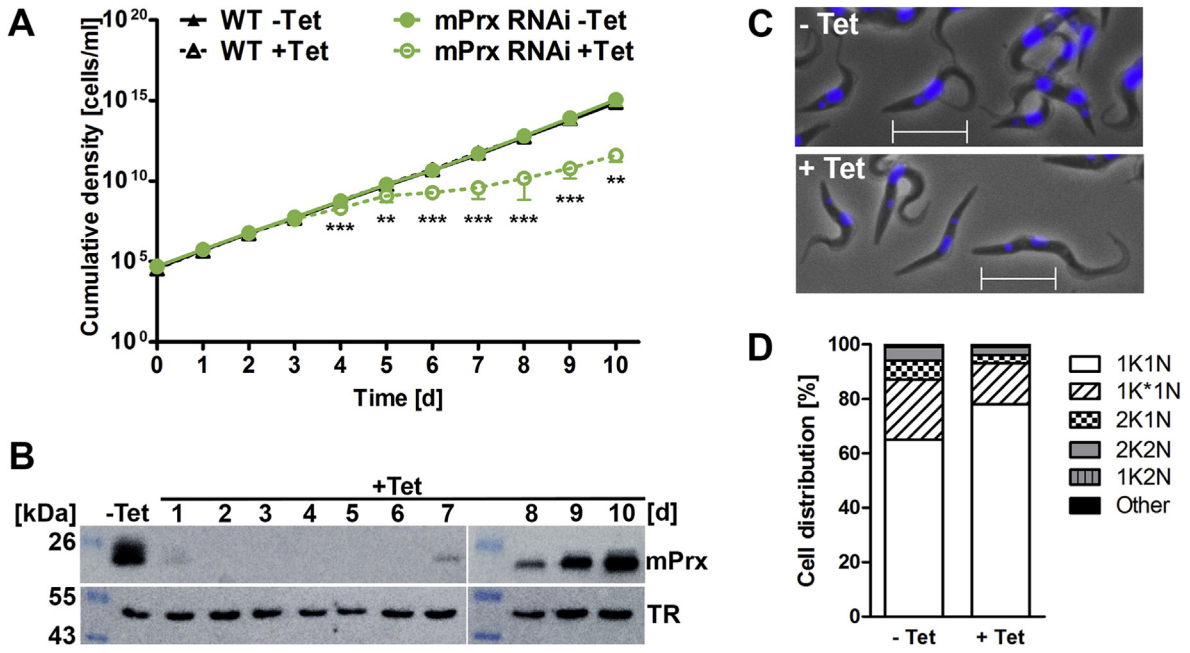

Fig. 3. PC mPrx-depleted cells have a proliferation defect, elongated morphology and signs of growth arrest in G1 phase. WT and mPrx RNAi cells were cultured ± Tet under standard conditions at 27 ˚C. (**A**) Cumulative cell density. The data for the mPrx RNAi cells are the mean ± SD from four different clones studied in parallel. They were analyzed by Microsoft Excel Student's standard unpaired *t*-test (**, $p \leq 0.01$; ***, $p \leq 0.001$). (**B**) Total lysates from 5×10^6 cells/lane harvested after different days (d) were subjected to Western blot analysis with antibodies against mPrx and TR as loading control. A representative analysis of one of four clones is depicted. (**C**) Fluorescence microscopy of mPrx RNAi cells cultured ± Tet for six days. Nuclear and kinetoplast DNA were visualized with DAPI (blue). Overlays of the phase contrast and DAPI images are depicted. Scale bar 10 μm. (**D**) Cell cycle analysis of the mPrx RNAi cells after six days ± Tet. K, kinetoplast; N, nucleus; 1K*1 N, cells with elongated kinetoplast and one nucleus. For each sample at least 800 parasites were inspected. (For interpretation of the references to colour in this figure legend, the reader is referred to the Web version of this article.)

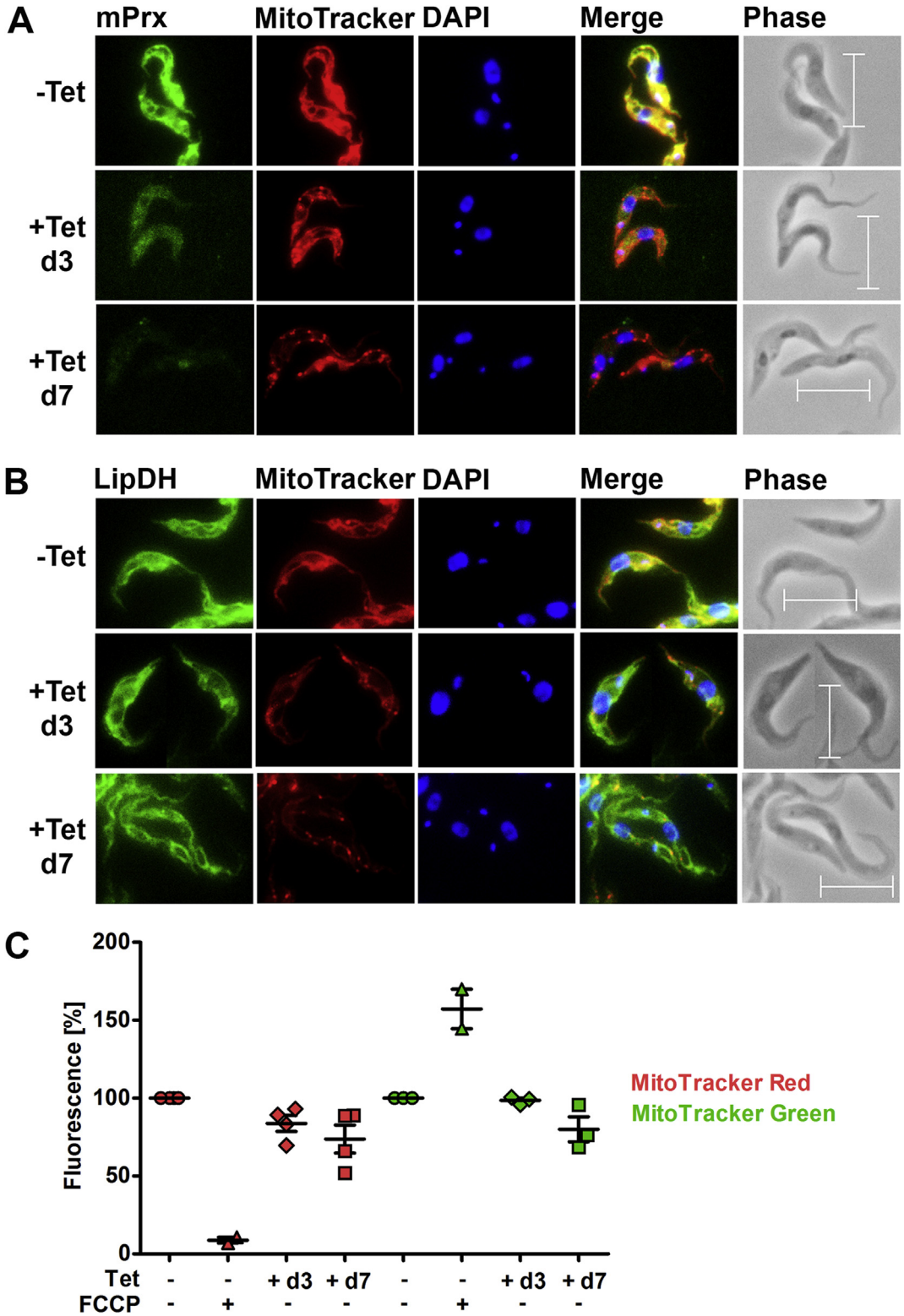

Fig. 4. PC mPrx-depleted *T. brucei* display decreased MitoTracker Red staining. The mPrx RNAi cells were grown ± Tet for three (d3) or seven (d7) days, stained with MitoTracker Red (red) and probed with antibodies against (**A**) mPrx or (**B**) LipDH (green). Nuclear and kinetoplast DNA were visualized by DAPI staining (blue). Merge, overlay of the three signals. Phase, phase contrast. Scale bar 10 μm. (**C**) The mPrx RNAi cells were cultured ± Tet for three or seven days, stained with MitoTracker Red or MitoTracker Green and subjected to flow cytometry. As control, non-induced cells were treated in parallel with FCCP. The values were normalized to the fluorescence observed for -Tet cells, which was set as 100%. The individual values from two to four independent analyses are depicted together with the mean ± SEM (standard error of the mean). (For interpretation of the references to colour in this figure legend, the reader is referred to the Web version of this article.)

are post-mitotic [48]. The induced cultures revealed a higher percentage of 1K1N cells compared to the non-induced controls (Fig. 3D). An increase of parasites with abnormal number of kinetoplasts or nuclei, as observed for various other mitochondrial RNAi cell lines [49], could not be detected. Taken together, PC *T. brucei* require mPrx for normal morphology and proliferation and appear to be prone to be arrested in the G1-phase of the cell cycle.

3.5. Depletion of mPrx affects the mitochondrial membrane potential of PC cells

Immunofluorescence microscopy of PC mPrx RNAi cells cultured with Tet for seven days confirmed the absence of the protein (Fig. 4A) and revealed an overall diminished MitoTracker Red staining together with a number of bright spots (Fig. 4A and B). Similar observations have been reported for PC cells that lack the mitochondrial acyl carrier protein (ACP) [50] or cardiolipin synthase [51]. In the latter case, the spots have been suggested to result from mitochondrial fragmentation. For the mPrx-depleted cells this is very unlikely since the matrix protein lipoamide dehydrogenase displayed a continuous mitochondrial distribution, independently if the parasites were cultured with or without Tet (Fig. 4B). Guler at al. propose that the MitoTracker bright spots in the ACP-depleted cells are at least partially due to localized regions of elevated mitochondrial membrane potential (ΔΨm) [50]. To study the impact of mPrx-depletion on the ΔΨm in more detail, we stained the cells with MitoTracker Red or MitoTracker Green and subjected them to flow cytometry (Fig. 4C). In parallel, non-induced cells were incubated with the dyes together with FCCP. In presence of the uncoupler, the MitoTracker Red signal was almost completely lost, whereas the MitoTracker Green signal was even increased. Such a phenomenon has been observed for cells that were simultaneously treated with the dye and FCCP [52]. The data indicated that MitoTracker Green staining in PC *T. brucei* is independent of ΔΨm as it is the case in many other cell types [52]. After three days of mPrx-depletion, the parasites showed a decreased MitoTracker Red signal but unchanged MitoTracker Green signal corroborating a lowered ΔΨm. In cells treated with Tet for seven days, the signals of both dyes were diminished which may suggest that their total mitochondrial mass is lowered. Another possibility is that in these proliferation, and probably also metabolically, arrested cells uptake and processing of the dyes are hampered. In summary, our data indicate that depletion of mPrx results in a decrease of ΔΨm.

3.6. mPrx reduces mitochondrially generated H_2O_2

Expression of a Tpx-coupled roGFP2 biosensor in the cytosol (Tpx-roGFP2) or mitochondrion (mito-roGFP2-Tpx) allows real-time measurements of the $T(SH)_2/TS_2$ ratio in intact PC cells [33]. In *T. brucei*, any known enzymatic hydroperoxide reduction is coupled to the trypanothione system and results in the transient formation of TS_2 and thus sensor oxidation (change in OxD). Subsequent regeneration of $T(SH)_2$ by TR restores the reduced sensor state. Recently, we demonstrated that mPrx takes part in the reduction of exogenously applied

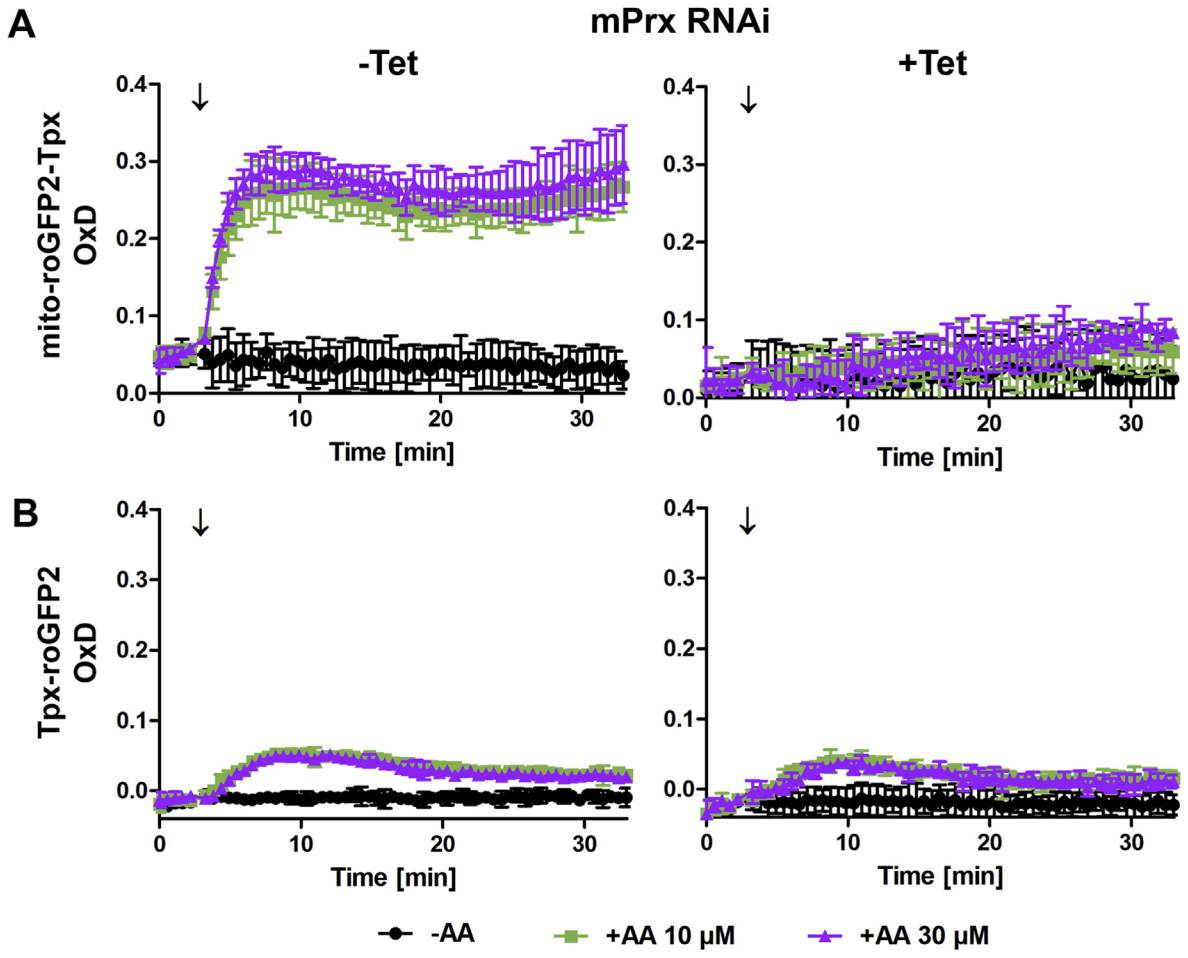

Fig. 5. Depletion of mPrx abolishes the response of the mito-roGFP2-Tpx sensor to antimycin A. PC mPrx RNAi cells expressing the Tpx-coupled roGFP2 sensor either in the (**A**) mitochondrion or (**B**) cytosol were cultured for three days -Tet (left graphs) or + Tet (right graphs) and then subjected to plate reader-based fluorescence measurements. The degree of sensor oxidation (OxD) was calculated as described in section 2.10. A single pulse of 10 or 30 µM antimycin A (+AA) or 0.3% DMSO alone (-AA) was given after 3 min (arrow). The data are the mean ± SD of three individual experiments with one clone. A second cell line showed identical results.

H_2O_2 [33]. Here we used antimycin A to generate H_2O_2 at the mitochondrion. The mito-roGFP2-Tpx/mPrx RNAi and Tpx-roGFP2/mPrx RNAi cells were pre-cultured ± Tet for three days and subjected to plate reader-based fluorescence measurements as described in section 2.10. (Fig. 5). In both, non-induced and induced mPrx RNAi cells, the basal OxD of the mito-roGFP2-Tpx was higher than that of the Tpx-roGFP2 sensor (Fig. 5A and B, black lines) indicating that the mitochondrion harbors a slightly less reducing milieu than the cytosol [33]. After injection of antimycin A, the cytosolic Tpx-roGFP2 displayed very minor oxidation. In contrast, the mito-roGFP2-Tpx sensor reported a marked increase in OxD and remained oxidized for the whole time of the experiment, suggesting a continuous, mainly mitochondrial, production of H_2O_2. In the mPrx depleted cells, the response of the mitochondrial sensor was almost abolished (Fig. 5A, right panel), whereas the low response of the cytosolic sensor was unaffected (Fig. 5B, right panel). These data place mPrx as the main enzyme responsible for the reduction of H_2O_2 in the mitochondrial matrix of PC *T. brucei*.

3.7. mPrx does not play a crucial role for the viability of PC cells in presence of oxidative stressors

To study if the peroxidase activity of mPrx is essential *in vivo*, we followed the viability and/or proliferation of the mPrx-depleted PC *T. brucei* in the presence of different H_2O_2-generating agents. In the first approach we used MitoParaquat, a mitochondria-targeted derivative of Paraquat that generates superoxide anions which are then converted into hydrogen peroxide [53]. MitoParaquat affected the proliferation of non-induced mPrx RNAi cells significantly, but, surprisingly, had only a minor additional effect on cells in which mPrx was depleted for two days and almost no effect on cells cultured + Tet for five days (Fig. 6A). Probably, in these proliferation-arrested cells with their diminished ΔΨm, the cationic compound is not properly enriched in the mitochondrion. In the second approach, we used antimycin A, a complex III inhibitor which generates superoxide anions in both the mitochondrial matrix and intermembrane space [54]. Also towards antimycin A, mPrx-depleted cells did not display an increased sensitivity when compared to the non-induced controls (Fig. 6B). Next, we treated the cells directly with H_2O_2. After 6 h of continous exposure to 10 μM H_2O_2, induced and non-induced mPrx RNAi cells started to die, and after 24 h, living cells were no longer detectable. Cells in which mPrx was depleted for seven days, appeared to be even slightly more resistant (Fig. 6C). Finally, we studied the short-term effect of high H_2O_2 concentrations. WT parasites as well as non-induced and induced mPrx RNAi cells were treated with 500 μM H_2O_2 for 30 min, stained with DCFH-DA and subjected to flow cytometry. The unstressed control cells displayed an identical low DCF fluorescence, indicating that the absence of mPrx does not lead to any cellular oxidative stress. After treatment with H_2O_2, WT parasites, non-induced mPrx RNAi cells and mPrx RNAi cells that were induced for only three days displayed marginally higher fluorescence. Most probably, the cells are still able to reduce H_2O_2. Remarkably, after seven days of mPrx depletion, highly fluorescent cells appeared (Fig. 6D), but an increase in dead cells was not observed. Most likely, these growth-arrested, and putatively also metabolically silenced, cells are unable to efficiently reduce exogenous H_2O_2, but obviously are not immediately damaged by the oxidant.

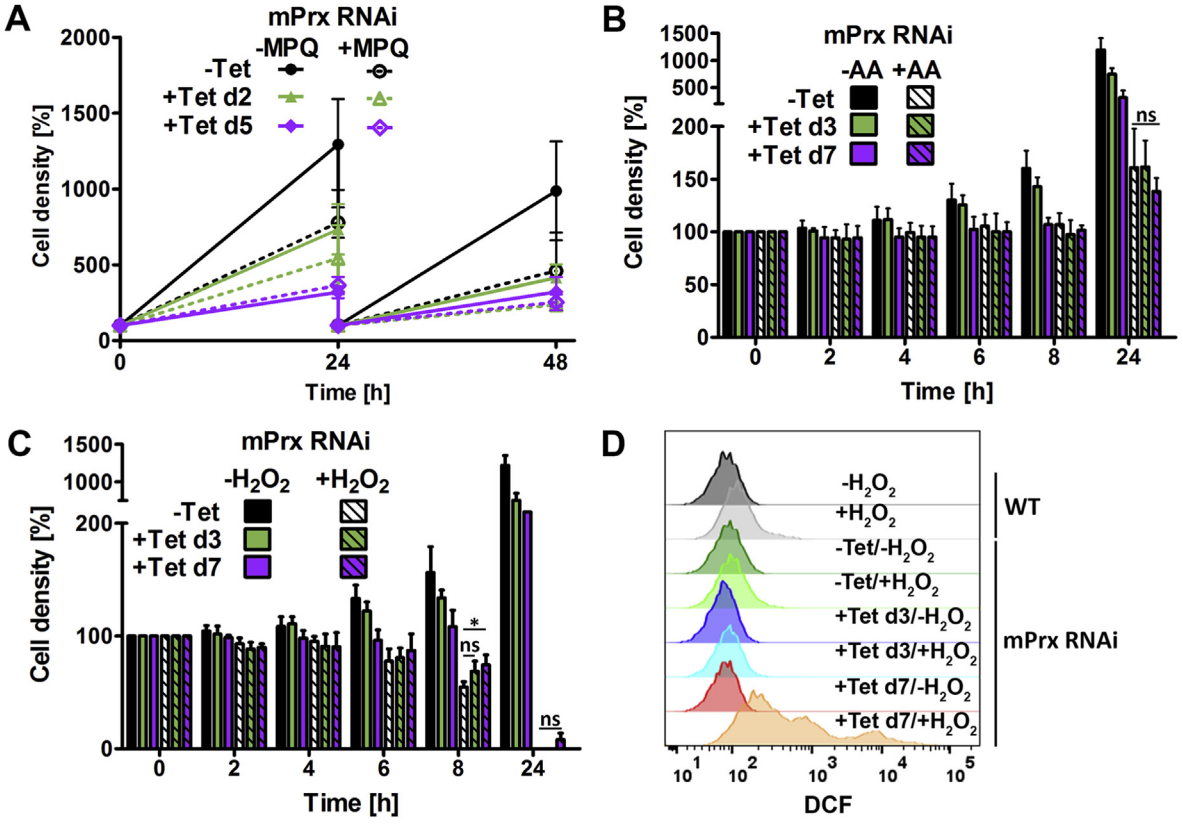

Fig. 6. PC mPrx-depleted cells do not show increased sensitivity towards oxidative stressors. The mPrx RNAi cells were pre-cultured ± Tet for (**A**) two and five (d2 and d5) or (**B** and **C**) three and seven (d3 and d7) days and then transferred into medium containing (**A**) ± Tet ± 10 μM MitoParaquat (MPQ), (**B**) ± Tet ± 10 μM antimycin A (AA) or (**C**) ± Tet ± 10 μM H_2O_2. After the indicated times, viable cells were counted. The data represent the mean ± SD from (**A** and **C**) one clone analyzed in three independent experiments or (**B**) two clones studied in parallel in two independent experiments. (**B–C**) The data were analyzed by standard unpaired *t*-test; ns, not significant ($p > 0.05$), *, $p \leq 0.05$. (**D**) WT parasites and mPrx RNAi cells cultured in the presence of Tet for three (d3) and seven (d7) days were treated with 500 μM H_2O_2 for 30 min, washed, stained with DCFH-DA and subjected to flow cytometry. A representative histogram from one of three independent experiments is depicted.

3.8. Treatment of PC T. brucei with H_2O_2 results in hyper-oxidation of cPrx and mPrx

Typical 2-Cys-Prxs are homodimers with each subunit harboring two redox-active cysteine residues. During catalysis, the peroxidative cysteine attacks a hydrogen peroxide molecule and is oxidized to a sulfenic acid which then reacts with the resolving cysteine of the second subunit under formation of an intersubunit disulfide bridge [55]. The reduced state of the enzyme is restored by reaction with an oxidoreductase such as a thioredoxin, or Tpx in the case of trypanosomatids. Under conditions of severe oxidative stress, a second hydrogen peroxide molecule can react with the sulfenic acid to a sulfinic or sulfonic acid. Hyper-oxidized Prxs are unable to form covalent dimers and lack peroxidase activity [4,56,57]. To get an insight into the susceptibility of the parasite Prxs to (hyper-)oxidation, we treated PC *T. brucei* with diamide or H_2O_2, disintegrated the cells in presence of NEM and subjected the lysates to Western blot analyses. As expected, under reducing conditions, both proteins run as monomer, independently of the treatment. Under non-reducing conditions, cells kept in PBS revealed cPrx largely in monomer form whereas a significant portion of mPrx was present as covalent dimer (Fig. S3A). Exposure of the cells to diamide shifted both proteins completely to the covalent dimer. The cPrx formed two species that likely represent dimers that are connected by either one or two intermolecular disulfide bridges, as previously seen in BS cells [58]. In the case of mPrx, a single band was visualized which run as the dimer in PBS-treated cells and probably represents the protein with the subunits linked by two disulfide bridges. In cells challenged with H_2O_2, both cPrx and mPrx were mainly present as monomer. This band reacted with the Prx-SO_3 antibodies which recognize the conserved active site of 2-Cys-Prxs with the peroxidative cysteine in the sulfinic or sulfonic state [59] (Fig. S3). A hyper-oxidized dimer, formed by human Prxs upon H_2O_2 treatment *in vitro* [56,60], was not observed. Unfortunately, due to the very similar size of cPrx and mature mPrx, the analysis did not allow to decide which of the two proteins was hyper-oxidized. Therefore we treated PC *T. brucei* with 100 μM H_2O_2 for 5 min and subjected the cell lysates to immunoprecipitation (IP) on anti-cPrx and anti-mPrx-agarose beads (section 2.11.), followed by Western blot analyses. The Prx-SO_3 antibodies revealed a band that migrated at the mass of the monomeric proteins in the input, flow through and elution fractions of both IPs (Fig. 7A and B, upper panel). The strong bands with higher masses in the elution fraction of the anti-cPrx beads (Fig. 7A, upper panel) are due to reaction of the anti-rabbit IgG antibodies with cPrx antibodies that partially elute from the beads upon boiling (not shown). Subsequent development of the cPrx IP membrane with cPrx antibodies detected the protein in the input and elution fractions (Fig. 7A, middle panel), but also the mPrx antibodies revealed

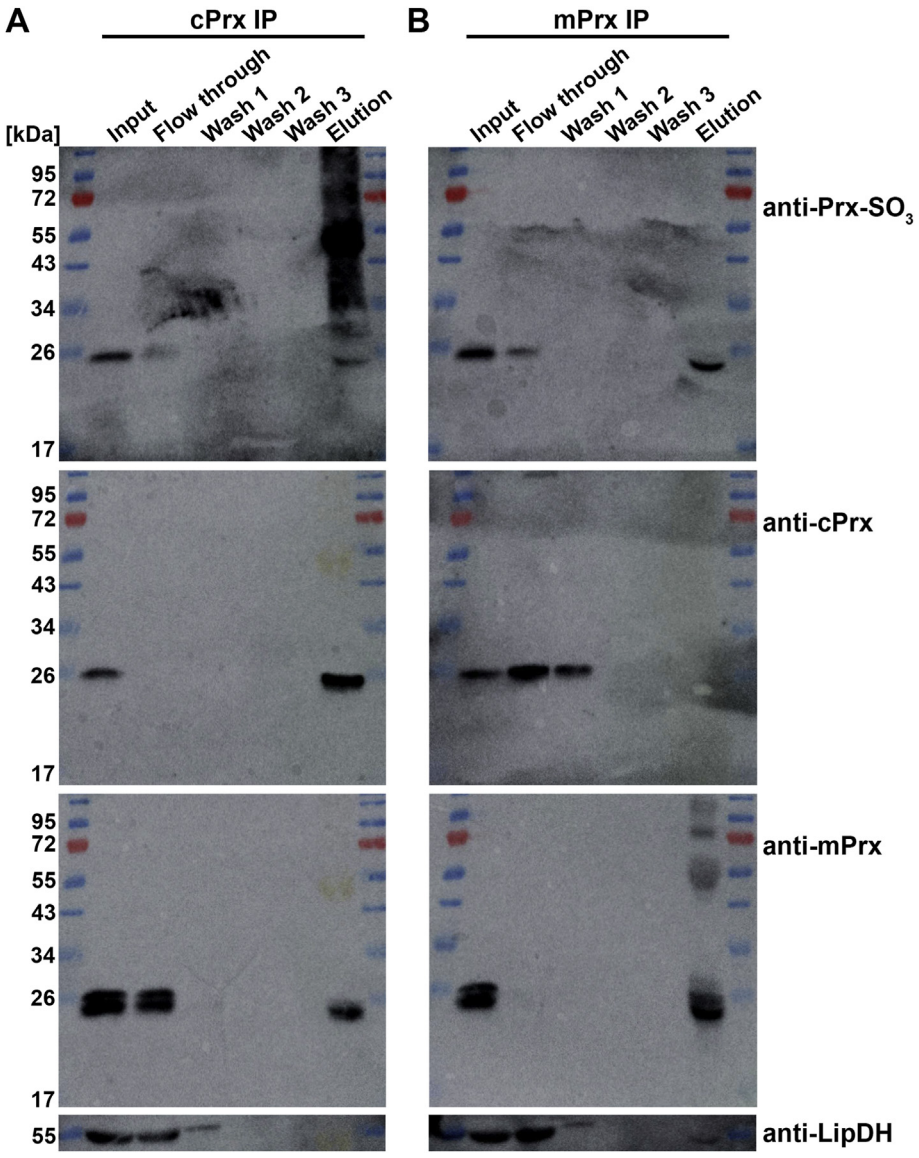

Fig. 7. Both cPrx and mPrx are sensitive to hyper-oxidation. PC *T. brucei* were incubated with 100 μM H_2O_2 for 5 min and lysed in the presence of 20 mM NEM. Lysates from about 4 × 10^8 cells (Input) were incubated with Protein A-agarose beads cross-linked to antibodies against (**A**) cPrx or (**B**) mPrx. After 4 h at 4 °C, the supernatants were removed (Flow through) and the beads were washed three times (Wash 1–3) and boiled in sample buffer (Elution). Aliquots corresponding to 10% of input, 10% of flow through, 5% of washes and the complete elution fraction were subjected to Western Blot analysis. The membranes were probed with antibodies against Prx-SO_3, stripped and reacted with anti-cPrx, followed by anti-mPrx antibodies. LipDH served as loading control.

some protein in the elution fraction (Fig. 7A, lower panel). Nevertheless, the fact that the flow through fraction of the mPrx IP reacted with both the Prx-SO_3 and cPrx antibodies, but not the mPrx antibodies showed that cPrx was hyper-oxidized. The mPrx IP was highly efficient. From these beads, exclusively mPrx was eluted (Fig. 7B, middle and lower panels). Taken together, under the conditions tested, both Prxs are prone to hyper-oxidation.

3.9. At 37 °C, mPrx-depleted PC T. brucei stop proliferation, but remain viable

As shown in Fig. 2A, BS mPrx-depleted cells lyse when the culture temperature is raised from 37 °C to 39 °C. To investigate if also PC *T. brucei* display a temperature-dependent phenotype, we studied the ability of mPrx-depleted cells to recover from a 1 h exposure to 41 °C, a condition shown to result in a reversible heat shock [61]. The treatment slightly affected the proliferation of WT parasites as well as the mPrx RNAi cells, independently if mPrx depletion was induced for two or five days (Fig. 8A). To follow the long-term heat sensitivity, we cultured the mPrx RNAi cells ± Tet for three days. Afterwards we kept the cells either at 27 °C or transferred them to 37 °C (Fig. 8B). Cultivation at 37 °C for 48 h or 72 h, caused a strong growth retardation of WT parasites and non-induced mPrx RNAi cells. The mPrx-depleted cells stopped proliferation almost completely, but, remarkably, did not lyse. Finally, we raised the temperature to 39 °C. Under these extreme conditions, all cells died at the same rate (Fig. 8C). Taken together, 37 °C heat stress amplifies the proliferation defect due to mPrx-depletion, but both effects appear to be additive.

3.10. Depletion of mPrx in PC cells does not result in the formation of protein aggregates

L. infantum promastigotes lacking mPrx display WT proliferation rate at 25 °C but a severe growth defect when cultivated at 37 °C [26] which is accompanied by higher levels of protein aggregates [27]. As mPrx-depleted PC *T. brucei* have a marked growth arrest already under standard culture conditions we asked if this may be due to formation of protein aggregates. WT parasites as well as non-induced and induced mPrx RNAi cells were lysed, soluble proteins were removed and the insoluble protein fraction subjected to SDS-PAGE (Fig. S4). All cells yielded a virtually identical pattern of weak bands. In contrast, when we exposed the cells to 39 °C for 24 h, a substantial level of aggregated proteins was observed. Again the pattern was identical for the three samples. In addition, under these conditions, the cells are highly damaged.

3.11. Expression and redox state of mPrx in PC T. brucei are independent of the growth phase and heat stress

When promastigote *L. donovani* are grown from early to late logarithmic and stationary phase, the cellular mPrx level increases dramatically [25]. To study if the expression of mPrx changes during growth of PC *T. brucei*, WT cells were harvested at a density of 1.7×10^6, 6.4×10^6 and 1.4×10^7 cells/ml, representing the early, mid and late logarithmic growth phase, respectively, lysed in presence of NEM and subjected to Western blot analysis. The mPrx antibodies visualized two bands corresponding to the monomer and covalent dimer under non-reducing conditions and a single monomer band under reducing conditions (Fig. S5A). The intensity and ratio of the bands were identical in the three samples.

To evaluate if heat stress affects the redox state of the parasite Prxs, PC *T. brucei* were grown at 27 °C (control) and at 37 °C for 24 and 48 h, lysed in presence of NEM and subjected to Western blot analysis. Prx-SO_3 antibodies did not visualize any specific band (Fig. S5B, upper panel). The cPrx and mPrx antibodies revealed for all three samples an identical level of the respective protein and the same monomer/dimer

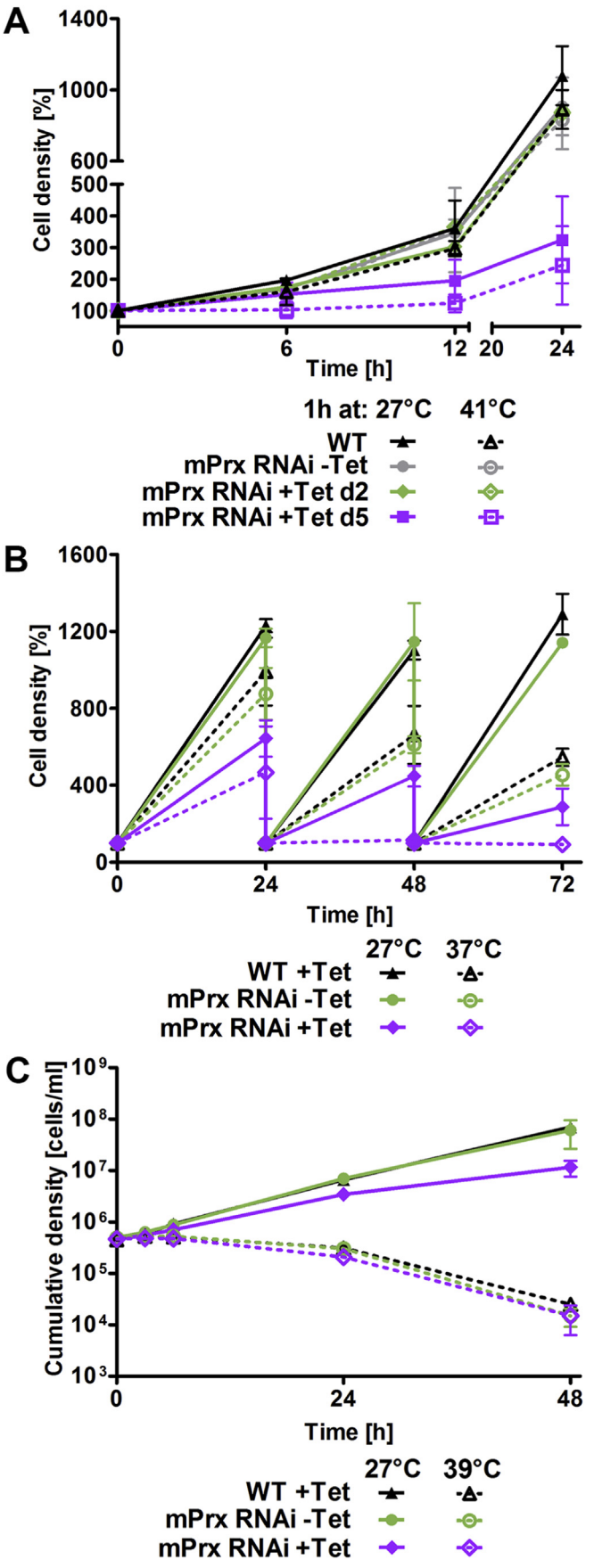

(caption on next page)

Fig. 8. Viability and proliferation of heat-stressed mPrx-depleted PC cells. (**A**) mPrx RNAi cells were pre-cultured with Tet for two (d2) or five (d5) days at 27 °C and split. One flask was further kept at 27 °C. The medium in the other flask was pre-heated to 41 °C, the cells were added and incubated for 1 h at 41 °C and then put back to 27 °C. Viable cells were counted after 6, 12 and 24 h. Non-induced cells and WT parasites were treated accordingly. The data are the mean ± SD from three independent experiments with one clone. A standard unpaired *t*-test did not reveal a significant difference between non-induced and induced mPrx RNAi cell lines ($p > 0.05$). (**B** and **C**) mPrx RNAi cells were cultured ± Tet for three days at 27 °C and subsequently in parallel at (**B**) 27 °C and 37 °C or (**C**) 27 °C and 39 °C. WT parasites + Tet were treated accordingly. (**B**) Every 24 h, viable cells were counted. The data are the mean ± SD from two clones studied in parallel in two independent experiments. (**C**) Viable cells were counted after 3, 6, 24, and 48 h. The graph shows the cumulative cell density of two experiments with WT parasites (mean) and two mPrxRNAi cell lines (mean ± SD). The cultures were diluted back to the starting density of 5×10^5 cells/ml, where appropriate.

ratio for mPrx (Fig. S5B, middle and lower panel). Thus, neither the expression nor the redox state of mPrx is affected by the growth stage and temperature corroborating the conclusion that the protein plays a constitutive role in PC *T. brucei*.

4. Discussion

BS *T. brucei* lacking either mPrx or the mitochondrial Px III proliferate almost as WT parasites and do not show an increased sensitivity towards exogenously applied hydrogen peroxide [10,14]. As both enzymes reduce hydrogen peroxide and thus display a partially overlapping *in vitro* substrate specificity, it has been proposed that only one of the two mitochondrial peroxidases might be required [10,22]. Here we show that BS *T. brucei* which lack Px III and are simultaneously depleted of mPrx do not have any significant growth defect. Both mitochondrial peroxidases are dispensable, at least under standard culture conditions. BS parasites possess a mitochondrion that lacks a functional electron transport chain (ETC) and generate ATP by glycolysis and maybe additional substrate-level phosphorylations in the mitochondrion [47,62]. Without an active respiratory chain, the mitochondrion probably does not constitute a significant source of oxidants. However, when the culture temperature is raised to 39 °C, mPrx-depleted BS cells are no longer viable. *L. infantum* mPrx (mTXNPx) is required for the survival of amastigote parasites in the mammalian host cell where it functions as heat-activated holdase [26]. The leishmanial protein has been proposed to facilitate the transition from insects to warm-blooded host environments [27,28]. In African trypanosomes, mPrx is not required for the adaptation of the parasites to the 37 °C body temperature of the mammalian host but may serve as a defense during fever episodes of the host acting as a heat-induced chaperone, similarly to its role in *Leishmania*.

In contrast to BS cells, PC *T. brucei* require mPrx for proliferation, in the absence of any stress. As reported recently, mPrx takes part in reducing exogenously applied hydrogen peroxide [33]. Here we show that treatment of PC cells with antimycin A has only a minor effect on the cytosolic $T(SH)_2/TS_2$ couple but results in marked oxidation of the mitochondrial trypanothione pool. The response is completely lost in cells lacking mPrx. This compares with yeast cells where H_2O_2-induced matrix glutathione oxidation is dependent on the presence of the mitochondrial Prx1 [63]. Thus, in PC *T. brucei*, antimycin A causes the generation of H_2O_2 primarily in the mitochondrial matrix and mPrx acts as H_2O_2-reducing peroxidase *in vivo*, in accordance with its *in vitro* activity. On the other hand, MitoParaquat, antimycin A and hydrogen peroxide affected the viability of PC *T. brucei* to the same degree, independently of the presence or absence of mPrx. This suggests that the peroxidase activity may not play a major physiological role, at least under culture conditions, in accordance with the situation in *Leishmania* [26]. Interestingly, in human neutrophils, the cytosolic Prx1 and Prx2 appear also to have a role that is not directly related to peroxide removal [64].

Hyper-oxidation of the peroxidative cysteine is a mechanism to activate the chaperone function of 2-Cys-Prxs [4]. Yet, the modification is not a prerequisite for the functional switch from a peroxidase to a chaperone. As shown in *Leishmania*, a mutant lacking the peroxidative cysteine fully rescues the *in vivo* infectivity of mPrx-depleted amastigote parasites [26–28]. This does, however, not exclude that hyper-oxidation of the parasite mPrx might be an additional chaperone-activating mechanism. In Jurkat cells that are exposed to 100 μM H_2O_2 for 10 min, 90% of the cytoplasmic hPrx1 and hPrx2, but only 10% of the mitochondrial hPrx3 are hyper-oxidized [56]. Here we treated PC *T. brucei* with 100 μM H_2O_2 for 5 min. Under these conditions, both cPrx and mPrx were modified suggesting that the parasite proteins are relatively sensitive to hyper-oxidation. As shown prevoiously, PC *T. brucei* that are exposed to 50 μM H_2O_2 for 20 min lose the ability to reduce cytosolic, but not mitochondrial, H_2O_2 [33] which indicates that prolonged exposure to H_2O_2 affects the cPrx to a higher degree. The lower sensitivity of mPrx towards hyper-oxidation may be due to the fact that it is more prone to covalent dimer formation than cPrx in intact PC *T. brucei*. This could at least partially be attributable to the less reducing environment in the mitochondrial matrix compared to the cytosol [33]. The sensitivity of human Prx1, Prx2 and Prx3 to hyper-oxidation is determined by the rate of disulfide bond formation between the peroxidative and resolving cysteines [56,57,60]. Typical mammalian 2-Cys-Prxs have been classified as hyper-oxidation-sensitive due to the presence of GGLG and C-terminal YF motifs which are absent in the resistant prokaryotic proteins [55]. However, even among mammalian Prxs, the susceptibility to hyper-oxidation and inactivation is remarkably variable. The mitochondrial hPrx3 is significantly more resilient to hyper-oxidation than hPrx1 and hPrx2 despite the fact that all three proteins exhibit a high degree of sequence identity and possess these motifs [56]. Recently two novel putative resistance-conferring motifs have been detected [65]. Both motifs are found in hPrx3 and the mPrx, but not cPrx, of *T. brucei*.

The growth defect of PC *T. brucei* caused by the depletion of mPrx starts with a delay and is accompanied by formation of long and thin cells that are probably arrested in the G1 phase of the cell cycle. The cells are able to resume proliferation after overcoming the RNAi regulation or upon Tet-removal (not shown), both conditions resulting in the re-appearance of mPrx. The phenotype was reminiscent of the late procyclic and mesocyclic stages which appear as the parasites migrate from the posterior to the anterior midgut of the tsetse fly [66]. The long mesocyclic trypomastigotes are G0/G1-phase arrested. When transferred back into *in vitro* culture medium they revert to the length of PC cells and resume growth [66]. Highly elongated PC *T. brucei* with a higher percentage of 1K1N cells that resemble mesocyclic trypomastigotes have been observed also upon depletion of the plasma membrane heme transporter [67]. Another example are parasites lacking Grx2, an oxidoreductase in the mitochondrial intermembrane space, which is also essential for proliferation of PC *T. brucei*. However, the latter cells do not show an altered DNA distribution and are unable to readapt normal proliferation [35]. RNAi knock-down of 101 predicted mitochondrial proteins in PC *T. brucei* resulted for 39 proteins in a strong or moderate growth retardation [49]. Several mutant cell lines displayed particularly long cells, and many of the cells had an abnormal K and N distribution pattern. The percentage of 1K1N was increased in only two cell lines, but lowered in all others [49]. Apparently, very different perturbations of the mitochondrial metabolism can affect the morphology, cell cycle progression and proliferation of PC *T. brucei*. Interestingly, silencing of Prx3 in breast cancer cells also inhibits proliferation and induces a cell cycle arrest in the G1 phase [68].

The depletion of mPrx did not affect the sensitivity towards exogenous H_2O_2 or the cellular redox status, as visualized by DCF staining, when compared to WT parasites. Moreover, the basal OxD reported by the cytosolic and mitochondrial Tpx-coupled roGFP2 sensors was

unaffected. These results indicate that the parasites are not subject to oxidative stress as result of mPrx down-regulation. Remarkably, upon long-term depletion of mPrx, the cells display strong DCF fluorescence when exposed to exogenous H_2O_2 but remain viable. Probably, these proliferation-arrested cells are unable to metabolize and thus accumulate H_2O_2, without being damaged directly by the oxidant.

The mPrx-depleted PC parasites have a diminished mitochondrial membrane potential. Similarly, depletion of Prx3 in HeLa cells enhances the decrease of the mitochondrial membrane potential induced by pro-apoptotic stimuli [69]. In *C. elegans*, repression of Prx3 leads to a lowered steady state level of ATP, impaired motility, and reduced brood size indicating the importance of the mitochondrial protein for normal life [70]. A recent study identified 171 mitochondrial proteins of *C. elegans* whose knock-down resulted in decreased mitochondrial membrane potential and induction of the mitochondrial unfolded protein response [71]. The proteins are involved in many processes; all of them are expected to either impair mitochondrial protein synthesis or import, or directly or indirectly influence the ETC. Very little is known about the response to mitochondrial stress in trypanosomes. A classical, transcription-controlled mechanism is unlikely as the parasites regulate their gene expression primarily on post-transcriptional levels [61]. Supplementing the medium with high glucose, to shift ATP generation to glycolysis, did not significantly improve the growth defect indicating that the energy metabolism is not primarily affected in the mPrx-depleted PC cells. The proliferation defect is not due to a general increase of aggregated proteins and also towards heat stress, the mPrx-depleted PC cell lines do not display a specific response. All our data suggest that mPrx plays a constitutive role in the insect stage of *T. brucei*. This is further corroborated by the finding that both the expression level and redox status of the protein are independent of the growth stage and culture temperature.

Qualitatively, the mitochondrial proteomes of BS and PC *T. brucei* are very similar, albeit, proteins of the TCA cycle and ETC often differ significantly when quantitative data are available [62]. The most obvious difference between the two developmental stages is the volume of the mitochondrion, which in PC cells occupies one fourth of the whole cell volume [72] and, most importantly, harbors an active ETC. In two immunoprecipitation studies on PC *T. brucei* that aimed at identification of the members of the translocase of the inner membrane (TIM) complex, which is essential for protein import into the mitochondrial matrix, mPrx was identified [73,74] which might suggest a transient interaction of mPrx with the TIM complex. Downregulation of TbTim17 or TbTim50 leads to growth retardation and decrease in mitochondrial membrane potential [75,76]; and the sensitivity of TbTim50-depleted cells towards H_2O_2 is even reduced [77]. Speculating that mPrx is involved in the import and/or folding of nuclear-encoded subunits of the respiratory chain complexes or other proteins whose shortage leads to a lowered mitochondrial membrane potential, long-term depletion of mPrx would be expected to affect the import of proteins into the mitochondrion. This may explain the gradual decrease of the mitochondrial membrane potential and increase of the proliferation defect observed and the fact that PC, but not BS, cells require mPrx under standard culture conditions.

5. Conclusions

The function of mPrx in *T. brucei* is dependent of the life cycle stage. In BS cells dwelling in the blood and body fluids of the mammalian hosts, mPrx is dispensable, even in cells simultaneously deficient in Px III. However, BS cells lacking mPrx die under conditions that mimic a fever situation suggesting that the protein functions as a heat-activated chaperone, similar to the protein in *Leishmania*. In contrast, in the PC insect stage, mPrx is required for proliferation in the absence of any stress. Prolonged depletion of mPrx results in an altered cell morphology, arrest of the cell cycle and diminished mitochondrial membrane potential. The data suggest that mPrx fulfills distinct functions as heat-activated and constitutive chaperone-like protein, respectively, in the malleable mitochondrion of *T. brucei*. Interesting aspects for future work could be to study the role of mPrx in BS parasites isolated from an infected natural host as well as to identify proteins that interact with mPrx in PC cells and to elucidate if these processes are thiol-(in)dependent.

Declaration of competing interest

The authors declare that there are no conflicts of interest.

Acknowledgments

We thank Catarina Lotsch and Vera Mitesser for their contributions to the cloning and kinetic analysis of the recombinant peroxidase. This work was supported by the Deutsche Forschungsgemeinschaft (Priority Programme SPP 1710 on “Dynamics of thiol-based redox switches in cellular physiology”, DFG Kr 1242/6–2).

Appendix A. Supplementary data

Supplementary data to this article can be found online at https://doi.org/10.1016/j.redox.2020.101547.

References

[1] G. Detienne, W. De Haes, L. Mergan, S.L. Edwards, L. Temmerman, S. Van Bael, Beyond ROS clearance: peroxiredoxins in stress signaling and aging, Ageing Res. Rev. 44 (2018) 33–48, https://doi.org/10.1016/j.arr.2018.03.005.
[2] S.G. Rhee, H.A. Woo, D. Kang, The role of peroxiredoxins in the transduction of H2O2 signals, Antioxidants Redox Signal. 28 (7) (2018) 537–557, https://doi.org/10.1089/ars.2017.7167.
[3] S. Stocker, K. Van Laer, A. Mijuskovic, T.P. Dick, The conundrum of hydrogen peroxide signaling and the emerging role of peroxiredoxins as redox relay hubs, Antioxidants Redox Signal. 28 (7) (2018) 558–573, https://doi.org/10.1089/ars.2017.7162.
[4] H.H. Jang, K.O. Lee, Y.H. Chi, B.G. Jung, S.K. Park, J.H. Park, J.R. Lee, S.S. Lee, J.C. Moon, J.W. Yun, Y.O. Choi, W.Y. Kim, J.S. Kang, G.W. Cheong, D.J. Yun, S.G. Rhee, M.J. Cho, S.Y. Lee, Two enzymes in one; two yeast peroxiredoxins display oxidative stress-dependent switching from a peroxidase to a molecular chaperone function, Cell 117 (5) (2004) 625–635, https://doi.org/10.1016/j.cell.2004.05.002.
[5] A.H. Fairlamb, P. Blackburn, P. Ulrich, B.T. Chait, A. Cerami, Trypanothione: a novel bis(glutathionyl)spermidine cofactor for glutathione reductase in trypanosomatids, Science 227 (4693) (1985) 1485–1487, https://doi.org/10.1126/science.3883489.
[6] R.L. Krauth-Siegel, A.E. Leroux, Low-molecular-mass antioxidants in parasites, Antioxidants Redox Signal. 17 (4) (2012) 583–607, https://doi.org/10.1089/ars.2011.4392.
[7] B. Manta, M. Bonilla, L. Fiestas, M. Sturlese, G. Salinas, M. Bellanda, M.A. Comini, Polyamine-based thiols in trypanosomatids: evolution, protein structural adaptations, and biological functions, Antioxidants Redox Signal. (2017), https://doi.org/10.1089/ars.2017.7133.
[8] B. Manta, M. Comini, A. Medeiros, M. Hugo, M. Trujillo, R. Radi, Trypanothione: a unique bis-glutathionyl derivative in trypanosomatids, Biochim. Biophys. Acta 1830 (5) (2013) 3199–3216, https://doi.org/10.1016/j.bbagen.2013.01.013.
[9] E. Tetaud, C. Giroud, A.R. Prescott, D.W. Parkin, D. Baltz, N. Biteau, T. Baltz, A.H. Fairlamb, Molecular characterisation of mitochondrial and cytosolic trypanothione-dependent tryparedoxin peroxidases in Trypanosoma brucei, Mol. Biochem. Parasitol. 116 (2) (2001) 171–183.
[10] S.R. Wilkinson, D. Horn, S.R. Prathalingam, J.M. Kelly, RNA interference identifies two hydroperoxide metabolizing enzymes that are essential to the bloodstream form of the African trypanosome, J. Biol. Chem. 278 (34) (2003) 31640–31646, https://doi.org/10.1074/jbc.M303035200.
[11] H. Hillebrand, A. Schmidt, R.L. Krauth-Siegel, A second class of peroxidases linked to the trypanothione metabolism, J. Biol. Chem. 278 (9) (2003) 6809–6815, https://doi.org/10.1074/jbc.M210392200.
[12] T. Schlecker, A. Schmidt, N. Dirdjaja, F. Voncken, C. Clayton, R.L. Krauth-Siegel, Substrate specificity, localization, and essential role of the glutathione peroxidase-type tryparedoxin peroxidases in Trypanosoma brucei, J. Biol. Chem. 280 (15) (2005) 14385–14394, https://doi.org/10.1074/jbc.M413338200.
[13] M. Bogacz, R.L. Krauth-Siegel, Tryparedoxin peroxidase-deficiency commits trypanosomes to ferroptosis-type cell death, Elife 7 (2018), https://doi.org/10.7554/eLife.37503.
[14] M. Diechtierow, R.L. Krauth-Siegel, A tryparedoxin-dependent peroxidase protects African trypanosomes from membrane damage, Free Radic. Biol. Med. 51 (4) (2011) 856–868, https://doi.org/10.1016/j.freeradbiomed.2011.05.014.

[15] C. Hiller, A. Nissen, D. Benitez, M.A. Comini, R.L. Krauth-Siegel, Cytosolic peroxidases protect the lysosome of bloodstream African trypanosomes from iron-mediated membrane damage, PLoS Pathog. 10 (4) (2014) e1004075, , https://doi.org/10.1371/journal.ppat.1004075.
[16] H. Castro, H. Budde, L. Flohe, B. Hofmann, H. Lunsdorf, J. Wissing, A.M. Tomas, Specificity and kinetics of a mitochondrial peroxiredoxin of Leishmania infantum, Free Radic. Biol. Med. 33 (11) (2002) 1563–1574, https://doi.org/10.1016/s0891-5849(02)01088-2.
[17] L. Thomson, A. Denicola, R. Radi, The trypanothione-thiol system in Trypanosoma cruzi as a key antioxidant mechanism against peroxynitrite-mediated cytotoxicity, Arch. Biochem. Biophys. 412 (1) (2003) 55–64.
[18] H. Castro, A.M. Tomas, Peroxidases of trypanosomatids, Antioxidants Redox Signal. 10 (9) (2008) 1593–1606, https://doi.org/10.1089/ars.2008.2050.
[19] R.L. Krauth-Siegel, M.A. Comini, Redox control in trypanosomatids, parasitic protozoa with trypanothione-based thiol metabolism, Biochim. Biophys. Acta 1780 (11) (2008) 1236–1248, https://doi.org/10.1016/j.bbagen.2008.03.006.
[20] C. Schaffroth, M. Bogacz, N. Dirdjaja, A. Nissen, R.L. Krauth-Siegel, The cytosolic or the mitochondrial glutathione peroxidase-type tryparedoxin peroxidase is sufficient to protect procyclic Trypanosoma brucei from iron-mediated mitochondrial damage and lysis, Mol. Microbiol. 99 (1) (2016) 172–187, https://doi.org/10.1111/mmi.13223.
[21] L.R. Krauth-Siegel, M.A. Comini, T. Schlecker, The trypanothione system, Subcell. Biochem. 44 (2007) 231–251, https://doi.org/10.1007/978-1-4020-6051-9_11.
[22] A.M. Tomas, H. Castro, Redox metabolism in mitochondria of trypanosomatids, Antioxidants Redox Signal. 19 (7) (2013) 696–707, https://doi.org/10.1089/ars.2012.4948.
[23] L. Piacenza, G. Peluffo, M.N. Alvarez, J.M. Kelly, S.R. Wilkinson, R. Radi, Peroxiredoxins play a major role in protecting Trypanosoma cruzi against macrophage- and endogenously-derived peroxynitrite, Biochem. J. 410 (2) (2008) 359–368, https://doi.org/10.1042/BJ20071138.
[24] J.P. Iyer, A. Kaprakkaden, M.L. Choudhary, C. Shaha, Crucial role of cytosolic tryparedoxin peroxidase in Leishmania donovani survival, drug response and virulence, Mol. Microbiol. 68 (2) (2008) 372–391, https://doi.org/10.1111/j.1365-2958.2008.06154.x.
[25] S. Harder, M. Bente, K. Isermann, I. Bruchhaus, Expression of a mitochondrial peroxiredoxin prevents programmed cell death in Leishmania donovani, Eukaryot. Cell 5 (5) (2006) 861–870, https://doi.org/10.1128/EC.5.5.861-870.2006.
[26] H. Castro, F. Teixeira, S. Romao, M. Santos, T. Cruz, M. Florido, R. Appelberg, P. Oliveira, F. Ferreira-da-Silva, A.M. Tomas, Leishmania mitochondrial peroxiredoxin plays a crucial peroxidase-unrelated role during infection: insight into its novel chaperone activity, PLoS Pathog. 7 (10) (2011) e1002325, , https://doi.org/10.1371/journal.ppat.1002325.
[27] F. Teixeira, H. Castro, T. Cruz, E. Tse, P. Koldewey, D.R. Southworth, A.M. Tomas, U. Jakob, Mitochondrial peroxiredoxin functions as crucial chaperone reservoir in Leishmania infantum, Proc. Natl. Acad. Sci. U. S. A. 112 (7) (2015) E616–E624, https://doi.org/10.1073/pnas.1419682112.
[28] F. Teixeira, E. Tse, H. Castro, K.A.T. Makepeace, B.A. Meinen, C.H. Borchers, L.B. Poole, J.C. Bardwell, A.M. Tomas, D.R. Southworth, U. Jakob, Chaperone activation and client binding of a 2-cysteine peroxiredoxin, Nat. Commun. 10 (1) (2019) 659, https://doi.org/10.1038/s41467-019-08565-8.
[29] M.D. Pineyro, D. Arias, A. Ricciardi, C. Robello, A. Parodi-Talice, Oligomerization dynamics and functionality of Trypanosoma cruzi cytosolic tryparedoxin peroxidase as peroxidase and molecular chaperone, Biochim. Biophys. Acta Gen. Subj. 1863 (10) (2019) 1583–1594, https://doi.org/10.1016/j.bbagen.2019.06.013.
[30] M. Yague-Capilla, D. Garcia-Caballero, F. Aguilar-Pereyra, V.M. Castillo-Acosta, L.M. Ruiz-Perez, A.E. Vidal, D. Gonzalez-Pacanowska, Base excision repair plays an important role in the protection against nitric oxide- and in vivo-induced DNA damage in Trypanosoma brucei, Free Radic. Biol. Med. 131 (2019) 59–71, https://doi.org/10.1016/j.freeradbiomed.2018.11.025.
[31] H. Schmidt, R.L. Krauth-Siegel, Functional and physicochemical characterization of the thioredoxin system in Trypanosoma brucei, J. Biol. Chem. 278 (47) (2003) 46329–46336, https://doi.org/10.1074/jbc.M305338200.
[32] A. Roldan, M.A. Comini, M. Crispo, R.L. Krauth-Siegel, Lipoamide dehydrogenase is essential for both bloodstream and procyclic Trypanosoma brucei, Mol. Microbiol. 81 (3) (2011) 623–639, https://doi.org/10.1111/j.1365-2958.2011.07721.x.
[33] S. Ebersoll, M. Bogacz, L.M. Gunter, T.P. Dick, R.L. Krauth-Siegel, A tryparedoxin-coupled biosensor reveals a mitochondrial trypanothione metabolism in trypanosomes, Elife 9 (2020), https://doi.org/10.7554/eLife.53227.
[34] S. Ceylan, V. Seidel, N. Ziebart, C. Berndt, N. Dirdjaja, R.L. Krauth-Siegel, The dithiol glutaredoxins of African trypanosomes have distinct roles and are closely linked to the unique trypanothione metabolism, J. Biol. Chem. 285 (45) (2010) 35224–35237, https://doi.org/10.1074/jbc.M110.165860.
[35] S. Ebersoll, B. Musunda, T. Schmenger, N. Dirdjaja, M. Bonilla, B. Manta, K. Ulrich, M.A. Comini, R.L. Krauth-Siegel, A glutaredoxin in the mitochondrial intermembrane space has stage-specific functions in the thermo-tolerance and proliferation of African trypanosomes, Redox Biol 15 (2018) 532–547, https://doi.org/10.1016/j.redox.2018.01.011.
[36] S.R. Wilkinson, M.C. Taylor, S. Touitha, I.L. Mauricio, D.J. Meyer, J.M. Kelly, TcGPXII, a glutathione-dependent Trypanosoma cruzi peroxidase with substrate specificity restricted to fatty acid and phospholipid hydroperoxides, is localized to the endoplasmic reticulum, Biochem. J. 364 (Pt 3) (2002) 787–794, https://doi.org/10.1042/BJ20020038.
[37] R. Schoneck, O. Billaut-Mulot, P. Numrich, M.A. Ouaissi, R.L. Krauth-Siegel, Cloning, sequencing and functional expression of dihydrolipoamide dehydrogenase from the human pathogen Trypanosoma cruzi, Eur. J. Biochem. 243 (3) (1997) 739–747.
[38] S. Biebinger, L.E. Wirtz, P. Lorenz, C. Clayton, Vectors for inducible expression of toxic gene products in bloodstream and procyclic Trypanosoma brucei, Mol. Biochem. Parasitol. 85 (1) (1997) 99–112.
[39] T. Schlecker, M.A. Comini, J. Melchers, T. Ruppert, R.L. Krauth-Siegel, Catalytic mechanism of the glutathione peroxidase-type tryparedoxin peroxidase of Trypanosoma brucei, Biochem. J. 405 (3) (2007) 445–454, https://doi.org/10.1042/BJ20070259.
[40] A.J. Meyer, T.P. Dick, Fluorescent protein-based redox probes, Antioxidants Redox Signal. 13 (5) (2010) 621–650, https://doi.org/10.1089/ars.2009.2948.
[41] T. Tomoyasu, A. Mogk, H. Langen, P. Goloubinoff, B. Bukau, Genetic dissection of the roles of chaperones and proteases in protein folding and degradation in the Escherichia coli cytosol, Mol. Microbiol. 40 (2) (2001) 397–413, https://doi.org/10.1046/j.1365-2958.2001.02383.x.
[42] H. Castro, S. Romao, F.R. Gadelha, A.M. Tomas, Leishmania infantum: provision of reducing equivalents to the mitochondrial tryparedoxin/tryparedoxin peroxidase system, Exp. Parasitol. 120 (4) (2008) 421–423, https://doi.org/10.1016/j.exppara.2008.09.002.
[43] A. Schmidt, C.E. Clayton, R.L. Krauth-Siegel, Silencing of the thioredoxin gene in Trypanosoma brucei brucei, Mol. Biochem. Parasitol. 125 (1–2) (2002) 207–210, https://doi.org/10.1016/S0166-6851(02)00215-3.
[44] S. Dean, J.D. Sunter, R.J. Wheeler, TrypTag.org: a trypanosome genome-wide protein localisation resource, Trends Parasitol. 33 (2) (2017) 80–82, https://doi.org/10.1016/j.pt.2016.10.009.
[45] R.B. Currier, K. Ulrich, A.E. Leroux, N. Dirdjaja, M. Deambrosi, M. Bonilla, Y.L. Ahmed, L. Adrian, H. Antelmann, U. Jakob, M.A. Comini, R.L. Krauth-Siegel, An essential thioredoxin-type protein of Trypanosoma brucei acts as redox-regulated mitochondrial chaperone, PLoS Pathog. 15 (9) (2019) e1008065, , https://doi.org/10.1371/journal.ppat.1008065.
[46] N. Lamour, L. Riviere, V. Coustou, G.H. Coombs, M.P. Barrett, F. Bringaud, Proline metabolism in procyclic Trypanosoma brucei is down-regulated in the presence of glucose, J. Biol. Chem. 280 (12) (2005) 11902–11910, https://doi.org/10.1074/jbc.M414274200.
[47] M. Mazet, P. Morand, M. Biran, G. Bouyssou, P. Courtois, S. Daulouede, Y. Millerioux, J.M. Franconi, P. Vincendeau, P. Moreau, F. Bringaud, Revisiting the central metabolism of the bloodstream forms of Trypanosoma brucei: production of acetate in the mitochondrion is essential for parasite viability, PLoS Neglected Trop. Dis. 7 (12) (2013) e2587, , https://doi.org/10.1371/journal.pntd.0002587.
[48] H. Zimmermann, I. Subota, C. Batram, S. Kramer, C.J. Janzen, N.G. Jones, M. Engstler, A quorum sensing-independent path to stumpy development in Trypanosoma brucei, PLoS Pathog. 13 (4) (2017) e1006324, , https://doi.org/10.1371/journal.ppat.1006324.
[49] D.E. Mbang-Benet, Y. Sterkers, L. Crobu, A. Sarrazin, P. Bastien, M. Pages, RNA interference screen reveals a high proportion of mitochondrial proteins essential for correct cell cycle progress in Trypanosoma brucei, BMC Genom. 16 (2015) 297, https://doi.org/10.1186/s12864-015-1505-5.
[50] J.L. Guler, E. Kriegova, T.K. Smith, J. Lukes, P.T. Englund, Mitochondrial fatty acid synthesis is required for normal mitochondrial morphology and function in Trypanosoma brucei, Mol. Microbiol. 67 (5) (2008) 1125–1142, https://doi.org/10.1111/j.1365-2958.2008.06112.x.
[51] M. Serricchio, P. Butikofer, An essential bacterial-type cardiolipin synthase mediates cardiolipin formation in a eukaryote, Proc. Natl. Acad. Sci. U. S. A. 109 (16) (2012) E954–E961, https://doi.org/10.1073/pnas.1121528109.
[52] W. Pendergrass, N. Wolf, M. Poot, Efficacy of MitoTracker Green and CMXrosamine to measure changes in mitochondrial membrane potentials in living cells and tissues, Cytometry 61 (2) (2004) 162–169, https://doi.org/10.1002/cyto.a.20033.
[53] E.L. Robb, J.M. Gawel, D. Aksentijevic, H.M. Cocheme, T.S. Stewart, M.M. Shchepinova, H. Qiang, T.A. Prime, T.P. Bright, A.M. James, M.J. Shattock, H.M. Senn, R.C. Hartley, M.P. Murphy, Selective superoxide generation within mitochondria by the targeted redox cycler MitoParaquat, Free Radic. Biol. Med. 89 (2015) 883–894, https://doi.org/10.1016/j.freeradbiomed.2015.08.021.
[54] S. Miwa, M.D. Brand, The topology of superoxide production by complex III and glycerol 3-phosphate dehydrogenase in Drosophila mitochondria, Biochim. Biophys. Acta 1709 (3) (2005) 214–219, https://doi.org/10.1016/j.bbabio.2005.08.003.
[55] Z.A. Wood, L.B. Poole, P.A. Karplus, Peroxiredoxin evolution and the regulation of hydrogen peroxide signaling, Science 300 (5619) (2003) 650–653, https://doi.org/10.1126/science.1080405.
[56] A.G. Cox, C.C. Winterbourn, M.B. Hampton, Mitochondrial peroxiredoxin involvement in antioxidant defence and redox signalling, Biochem. J. 425 (2) (2009) 313–325, https://doi.org/10.1042/BJ20091541.
[57] A.C. Haynes, J. Qian, J.A. Reisz, C.M. Furdui, W.T. Lowther, Molecular basis for the resistance of human mitochondrial 2-Cys peroxiredoxin 3 to hyperoxidation, J. Biol. Chem. 288 (41) (2013) 29714–29723, https://doi.org/10.1074/jbc.M113.473470.
[58] K. Ulrich, C. Finkenzeller, S. Merker, F. Rojas, K. Matthews, T. Ruppert, R.L. Krauth-Siegel, Stress-induced protein S-glutathionylation and S-trypanothionylation in African trypanosomes-A quantitative redox proteome and thiol analysis, Antioxidants Redox Signal. 27 (9) (2017) 517–533, https://doi.org/10.1089/ars.2016.6947.
[59] T.S. Chang, W. Jeong, H.A. Woo, S.M. Lee, S. Park, S.G. Rhee, Characterization of mammalian sulfiredoxin and its reactivation of hyperoxidized peroxiredoxin through reduction of cysteine sulfinic acid in the active site to cysteine, J. Biol. Chem. 279 (49) (2004) 50994–51001, https://doi.org/10.1074/jbc.M409482200.
[60] J. Dalla Rizza, L.M. Randall, J. Santos, G. Ferrer-Sueta, A. Denicola, Differential parameters between cytosolic 2-Cys peroxiredoxins, PRDX1 and PRDX2, Protein Sci. 28 (1) (2019) 191–201, https://doi.org/10.1002/pro.3520.
[61] S. Kramer, R. Queiroz, L. Ellis, H. Webb, J.D. Hoheisel, C. Clayton, M. Carrington,

Heat shock causes a decrease in polysomes and the appearance of stress granules in trypanosomes independently of eIF2(alpha) phosphorylation at Thr169, J. Cell Sci. 121 (Pt 18) (2008) 3002–3014, https://doi.org/10.1242/jcs.031823.

[62] A. Zikova, Z. Verner, A. Nenarokova, P.A.M. Michels, J. Lukes, A paradigm shift: the mitoproteomes of procyclic and bloodstream Trypanosoma brucei are comparably complex, PLoS Pathog. 13 (12) (2017) e1006679, , https://doi.org/10.1371/journal.ppat.1006679.

[63] G. Calabrese, E. Peker, P.S. Amponsah, M.N. Hoehne, T. Riemer, M. Mai, G.P. Bienert, M. Deponte, B. Morgan, J. Riemer, Hyperoxidation of mitochondrial peroxiredoxin limits H2 O2 -induced cell death in yeast, EMBO J. 38 (18) (2019) e101552, , https://doi.org/10.15252/embj.2019101552.

[64] L.F. de Souza, A.G. Pearson, P.E. Pace, A.L. Dafre, M.B. Hampton, F.C. Meotti, C.C. Winterbourn, Peroxiredoxin expression and redox status in neutrophils and HL-60cells, Free Radic. Biol. Med. 135 (2019) 227–234, https://doi.org/10.1016/j.freeradbiomed.2019.03.007.

[65] J.A. Bolduc, K.J. Nelson, A.C. Haynes, J. Lee, J.A. Reisz, A.H. Graff, J.E. Clodfelter, D. Parsonage, L.B. Poole, C.M. Furdui, W.T. Lowther, Novel hyperoxidation resistance motifs in 2-Cys peroxiredoxins, J. Biol. Chem. 293 (30) (2018) 11901–11912, https://doi.org/10.1074/jbc.RA117.001690.

[66] J. Van Den Abbeele, Y. Claes, D. van Bockstaele, D. Le Ray, M. Coosemans, Trypanosoma brucei spp. development in the tsetse fly: characterization of the post-mesocyclic stages in the foregut and proboscis, Parasitology 118 (Pt 5) (1999) 469–478, https://doi.org/10.1017/s0031182099004217.

[67] E. Horakova, P. Changmai, M. Vancova, R. Sobotka, J. Van Den Abbeele, B. Vanhollebeke, J. Lukes, The Trypanosoma brucei TbHrg protein is a heme transporter involved in the regulation of stage-specific morphological transitions, J. Biol. Chem. 292 (17) (2017) 6998–7010, https://doi.org/10.1074/jbc.M116.762997.

[68] P.J. Chua, E.H. Lee, Y. Yu, G.W. Yip, P.H. Tan, B.H. Bay, Silencing the peroxiredoxin III gene inhibits cell proliferation in breast cancer, Int. J. Oncol. 36 (2) (2010) 359–364.

[69] T.S. Chang, C.S. Cho, S. Park, S. Yu, S.W. Kang, S.G. Rhee, Peroxiredoxin III, a mitochondrion-specific peroxidase, regulates apoptotic signaling by mitochondria, J. Biol. Chem. 279 (40) (2004) 41975–41984, https://doi.org/10.1074/jbc.M407707200.

[70] M. Ranjan, J. Gruber, L.F. Ng, B. Halliwell, Repression of the mitochondrial peroxiredoxin antioxidant system does not shorten life span but causes reduced fitness in Caenorhabditis elegans, Free Radic. Biol. Med. 63 (2013) 381–389, https://doi.org/10.1016/j.freeradbiomed.2013.05.025.

[71] S.G. Rolland, S. Schneid, M. Schwarz, E. Rackles, C. Fischer, S. Haeussler, S.G. Regmi, A. Yeroslaviz, B. Habermann, D. Mokranjac, E. Lambie, B. Conradt, Compromised mitochondrial protein import acts as a signal for UPR(mt), Cell Rep. 28 (7) (2019) 1659–1669, https://doi.org/10.1016/j.celrep.2019.07.049 e1655.

[72] S. Bohringer, H. Hecker, Quantitative ultrastructural investigations of the life cycle of Trypanosoma brucei: a morphometric analysis, J. Protozool. 22 (4) (1975) 463–467.

[73] A. Harsman, A. Schneider, Mitochondrial protein import in trypanosomes: expect the unexpected, Traffic 18 (2) (2017) 96–109, https://doi.org/10.1111/tra.12463.

[74] J.T. Smith Jr., U.K. Singha, S. Misra, M. Chaudhuri, Divergent small tim homologues are associated with TbTim17 and critical for the biogenesis of TbTim17 protein complexes in trypanosoma brucei, mSphere 3 (3) (2018), https://doi.org/10.1128/mSphere.00204-18.

[75] M.R. Duncan, M. Fullerton, M. Chaudhuri, Tim50 in Trypanosoma brucei possesses a dual specificity phosphatase activity and is critical for mitochondrial protein import, J. Biol. Chem. 288 (5) (2013) 3184–3197, https://doi.org/10.1074/jbc.M112.436378.

[76] U.K. Singha, E. Peprah, S. Williams, R. Walker, L. Saha, M. Chaudhuri, Characterization of the mitochondrial inner membrane protein translocator Tim17 from Trypanosoma brucei, Mol. Biochem. Parasitol. 159 (1) (2008) 30–43, https://doi.org/10.1016/j.molbiopara.2008.01.003.

[77] M. Fullerton, U.K. Singha, M. Duncan, M. Chaudhuri, Down regulation of Tim50 in Trypanosoma brucei increases tolerance to oxidative stress, Mol. Biochem. Parasitol. 199 (1–2) (2015) 9–18, https://doi.org/10.1016/j.molbiopara.2015.03.002.